The Protozoan Parasite Toxoplasma gondii Selectively Reprograms the Host Cell Translatome

Leroux, Louis-Philippe; Lorent, Julie; Graber, Tyson E.; Chaparro, Visnu; Masvidal, Laia; Aguirre, Maria; Fonseca, Bruno D.; van Kempen, Léon C.; Alain, Tommy; Larsson, Ola

Published in:
Infection and Immunity

DOI:
10.1128/IAI.00244-18

Publication date:
2018

AMERICAN SOCIETY FOR MICROBIOLOGY | Infection and Immunity®

CELLULAR MICROBIOLOGY:
PATHOGEN-HOST CELL MOLECULAR INTERACTIONS

The Protozoan Parasite *Toxoplasma gondii* Selectively Reprograms the Host Cell Translatome

Louis-Philippe Leroux,[a,b] Julie Lorent,[c] Tyson E. Graber,[d] Visnu Chaparro,[a,b] Laia Masvidal,[c] Maria Aguirre,[e] Bruno D. Fonseca,[d] Léon C. van Kempen,[e,f,g] Tommy Alain,[d] Ola Larsson,[c] Maritza Jaramillo[a,b]

[a]Institut National de la Recherche Scientifique-Institut Armand Frappier, Laval, Quebec, Canada
[b]Centre for Host-Parasite Interactions, Institut National de la Recherche Scientifique-Institut Armand Frappier, Laval, Quebec, Canada
[c]Department of Oncology-Pathology, Science for Life Laboratory, Karolinska Institutet, Stockholm, Sweden
[d]Children's Hospital of Eastern Ontario Research Institute, Department of Biochemistry, Microbiology and Immunology, University of Ottawa, Ottawa, Ontario, Canada
[e]Lady Davis Institute, Jewish General Hospital, Montreal, Quebec, Canada
[f]Department of Pathology, McGill University, Montreal, Quebec, Canada
[g]Department of Pathology and Medical Biology, University Medical Centre, Groningen, The Netherlands

ABSTRACT The intracellular parasite *Toxoplasma gondii* promotes infection by targeting multiple host cell processes; however, whether it modulates mRNA translation is currently unknown. Here, we show that infection of primary murine macrophages with type I or II *T. gondii* strains causes a profound perturbation of the host cell translatome. Notably, translation of transcripts encoding proteins involved in metabolic activity and components of the translation machinery was activated upon infection. In contrast, the translational efficiency of mRNAs related to immune cell activation and cytoskeleton/cytoplasm organization was largely suppressed. Mechanistically, *T. gondii* bolstered mechanistic target of rapamycin (mTOR) signaling to selectively activate the translation of mTOR-sensitive mRNAs, including those with a 5′-terminal oligopyrimidine (5′ TOP) motif and those encoding mitochondrion-related proteins. Consistent with parasite modulation of host mTOR-sensitive translation to promote infection, inhibition of mTOR activity suppressed *T. gondii* replication. Thus, selective reprogramming of host mRNA translation represents an important subversion strategy during *T. gondii* infection.

KEYWORDS *Toxoplasma gondii*, host-pathogen interactions, mTOR, macrophages, translational control

Toxoplasma gondii, the causative agent of toxoplasmosis, is an obligate intracellular protozoan parasite that invades virtually all nucleated cells (1) and infects a remarkably diverse range of vertebrate hosts, including humans and mice (2, 3). Although toxoplasmosis is generally asymptomatic, reactivation of encysted parasites can lead to deleterious consequences for immunosuppressed individuals (1, 4). Furthermore, congenital toxoplasmosis can cause spontaneous abortion or severe birth defects (5). To replicate, *T. gondii* hijacks host cell organelles and scavenges nutrients (6, 7). In addition, the parasite targets signaling pathways and affects host cell transcription to subvert immune functions, promote host cell survival, and modulate host cell processes to favor its own replication (7–9). Despite this body of evidence, how *T. gondii* modulates host cell protein synthesis remains unknown.

Translational control allows cells to rapidly change their proteome to respond to external triggers or other cues without *de novo* mRNA synthesis (10, 11). In fact, modulation of translational efficiency represents a critical mechanism in a plethora of biological processes, such as cell differentiation, metabolism, growth, and proliferation

Received 29 March 2018 **Returned for modification** 1 May 2018 **Accepted** 22 June 2018

Accepted manuscript posted online 2 July 2018

Citation Leroux L-P, Lorent J, Graber TE, Chaparro V, Masvidal L, Aguirre M, Fonseca BD, van Kempen LC, Alain T, Larsson O, Jaramillo M. 2018. The protozoan parasite *Toxoplasma gondii* selectively reprograms the host cell translatome. Infect Immun 86:e00244-18. https://doi.org/10.1128/IAI.00244-18.

Editor John H. Adams, University of South Florida

Address correspondence to Maritza Jaramillo, maritza.jaramillo@iaf.inrs.ca.

J.L. and T.E.G. equally contributed to this work.

(10, 12–14). Accordingly, dysregulation of mRNA translation is a hallmark of various types of cancer (15, 16) and other clinical disorders, such as inflammatory airway pathologies (17), fibrosis (18), and neurodegenerative diseases (19–22). In eukaryotes, translation is mainly regulated at the initiation step, during which ribosomes are recruited to the mRNA, a process which can be modulated via multiple mechanisms. For instance, the association of mRNAs with RNA-binding proteins (23) and the presence of features including the 5′-terminal oligopyrimidine (5′ TOP) motif (24) or structured sequence motifs within the 5′ untranslated region (UTR) of mRNA (25) represent regulatory mechanisms selectively influencing translational efficiency. Notably, ribosome recruitment is facilitated by the recognition of the mRNA 5′-m^7G cap structure by eukaryotic initiation factor 4E (eIF4E), which, together with the scaffold protein eIF4G and the RNA helicase eIF4A, forms the eIF4F complex (26). Assembly of the eIF4F complex is prevented by eIF4E-binding proteins (4E-BPs), which block the eIF4E-eIF4G interaction and eIF4F formation (27, 28). Hyperphosphorylation of 4E-BPs by the serine/threonine kinase mechanistic target of rapamycin (mTOR) complex 1 (mTORC1) leads to a reduction of the 4E-BPs' affinity for eIF4E, which favors the eIF4E-eIF4G interaction and the initiation of translation (29). Thus, signaling through the mTORC1 axis is pivotal for translational control.

Regulation of mRNA translation efficiency is required for normal immune functions (30) and is altered during infection (31, 32). mTORC1 and its downstream targets 4E-BP1/4E-BP2 and S6K1/S6K2 are key components of the innate immune response (33–37). Accordingly, changes in mTORC1 signaling are linked to subversion of host mRNA translation by viruses (38, 39), bacteria (40, 41), and the protozoan parasite *Leishmania major* (42).

With regard to toxoplasmosis, translational control has been assessed only in the parasite (43, 44); however, how the parasite modulates host cell translation is unknown. Here, we report that *T. gondii* selectively reprograms the translational landscape of the host cell to promote its replication. Through a nonbiased approach (i.e., transcriptome-wide polysome profiling), we identified a large number of transcripts whose translation efficiency is modulated upon infection (i.e., activated or repressed). In addition, we show that selective activation of host mRNA translation by *T. gondii* is mTOR sensitive and is associated with the presence of distinct motifs in the 5′ UTRs of identified transcripts. Accordingly, inhibition of mTOR activity dampens parasite replication. Overall, this study provides evidence that selective regulation of host mRNA translation contributes to *T. gondii* survival.

RESULTS

***Toxoplasma gondii* increases protein synthesis in infected macrophages.** During infectious diseases, translational control can act as a host defense mechanism but also can be exploited by the invading pathogen as a survival strategy (30–32). To explore these possibilities during *T. gondii* infection, we inoculated bone marrow-derived murine macrophages (BMDM) with the RH (type I) and ME49 (type II) strains and assessed their effects on global protein synthesis by comparing the amounts of monosomes (inefficient translation) and heavy polysomes (efficient translation), as observed from polysome tracings. This approach revealed an increase in the amount of heavy polysomes with a concomitant decrease in the amount of monosomes in *T. gondii*-infected cells (Fig. 1A, left). The ratio of the normalized absorbance (254 nm) of heavy polysomes to monosomes indicated that type I and II strains enhance host cell protein synthesis to similar extents (mean fold changes over the value for the uninfected control [standard deviations {SD}] of 1.59 [0.19] for RH and 1.60 [0.11] for ME49) (Fig. 1A, right). These observed differences did not result from a contaminating signal originating from the parasite, as polysome tracings from *T. gondii* tachyzoites alone were barely detected (see Fig. S1A in the supplemental material). Thus, *T. gondii* infection leads to increased macrophage protein synthesis.

***T. gondii* infection causes selective modulation of host cell translation.** The increased amount of mRNA associated with heavy polysomes following parasite infec-

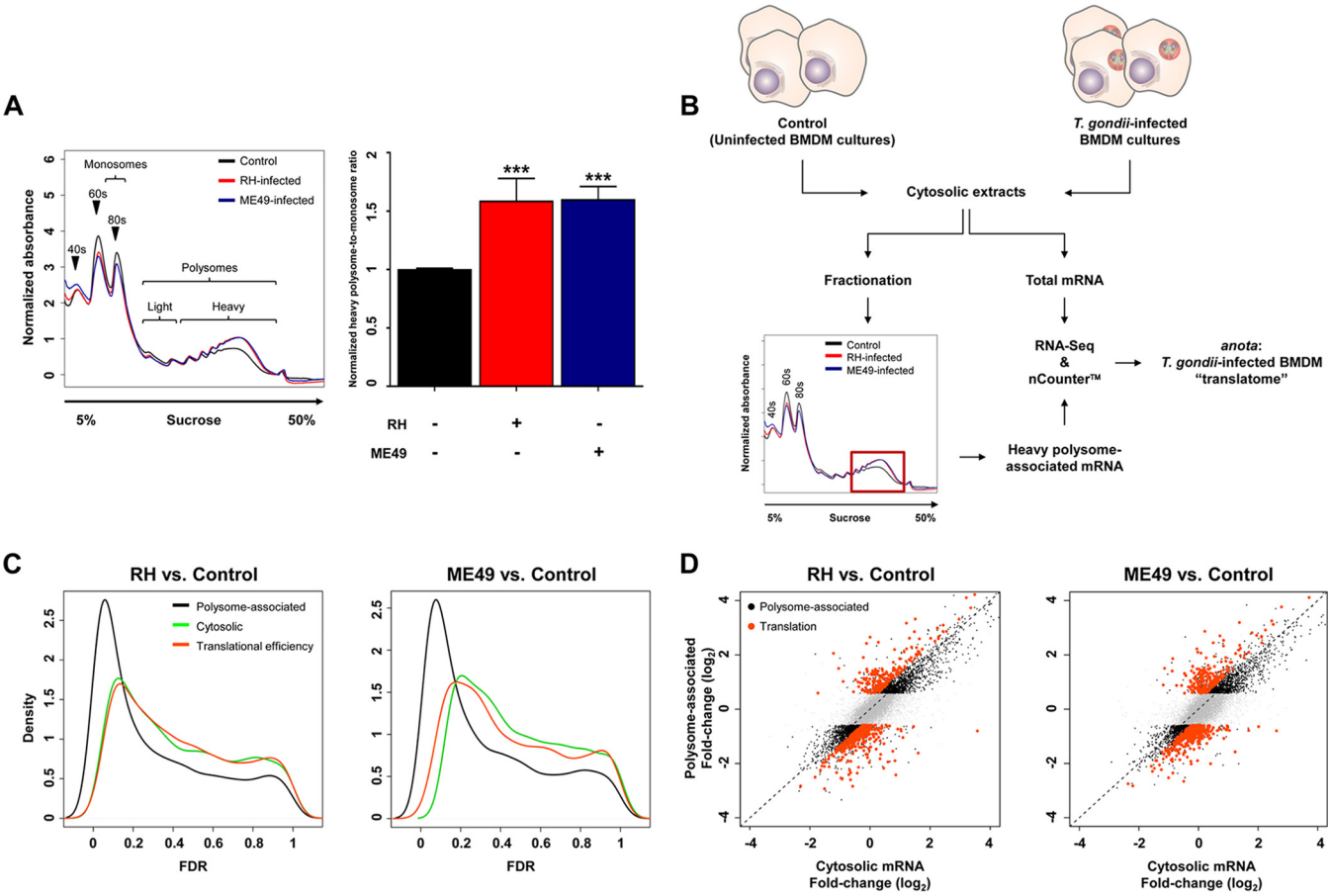

FIG 1 *T. gondii* infection stimulates protein synthesis and selectively modulates translational efficiencies in BMDM. (A) BMDM cultures were inoculated with either RH or ME49 *T. gondii* tachyzoites (MOI of 3:1) or left uninfected (control) for 8 h. Cell lysates were sedimented on 5 to 50% sucrose gradients. (Left) Gradients were fractionated, and the absorbance at 254 nm was recorded continuously. Absorbance values were normalized. Arrows indicate the 40S and 60S ribosomal subunits and 80S (monosomes). The light and heavy polysome regions were identified as fractions containing mRNA associated with 2 to 3 and >3 ribosomes, respectively. Polysome tracings are representative of data from at least four independent experiments. (Right) The area under the curve of the monosome and heavy polysome regions was calculated, and the heavy polysome-to-monosome ratios were then normalized to values for uninfected BMDM cultures (control) (means [SD]; $n = 4$ biological replicates). (B) Workflow strategy to characterize the translatome of *T. gondii*-infected BMDM. Cytosolic extracts from control (uninfected) and *T. gondii*-infected (RH or ME49) BMDM cultures were sedimented on a sucrose gradient. Heavy polysome fractions were pooled (referred to as heavy polysome-associated mRNA). Total and heavy polysome-associated mRNAs were sequenced by RNA-Seq and analyzed by ANOTA, an R package ($n = 3$ biological replicates). Validation of genes identified by RNA-Seq was accomplished with targeted nCounter assays (custom panel; $n = 3$ biological replicates). (C) Densities of FDRs for changes in polysome-associated mRNA, cytosolic mRNA, or translational efficiency (i.e., following ANOTA) for each strain compared to the uninfected control. (D) Scatter plots of $\log_2$ fold changes (for the same comparisons as in panel B) for polysome-associated and cytosolic mRNAs. Transcripts showing altered translational efficiencies and mRNAs showing a changed polysome association (which can be explained by altered cytosolic mRNA levels following, e.g., modulated transcription) are indicated. (C and D) Data analyses were performed on samples generated from three independent biological replicates.

tion is consistent with parasite-induced mRNA-selective and/or global changes in host cell translational efficiency. To resolve the selective regulation of translational efficiency, we used polysome profiling, quantified by transcriptome sequencing (RNA-Seq) (Fig. 1B). During polysome profiling, both efficiently translated mRNA (defined here as mRNA associated with >3 ribosomes) and cytosolic mRNA (input) are isolated and quantified. As altered cytosolic mRNA levels will lead to corresponding changes in polysome-associated mRNA even without a modulation of translational efficiency, differences in polysome-associated mRNA levels require adjustment for changes in cytosolic mRNA levels to identify bona fide changes in translational efficiency. Here, we used the ANOTA (analysis of translational activity) algorithm for this purpose (45). Polysome profiling coupled with ANOTA of uninfected and RH- or ME49-infected BMDM revealed widespread selective alterations in translational efficiency upon infection with either strain (Fig. 1C). In total, 322 and 625 mRNAs showed activated and repressed translational efficiencies, respectively, in response to either strain (false

discovery rate [FDR] of ≤0.25) (Fig. 1D; see also Table S1 in the supplemental material). In contrast, only 51 targets showed translational efficiencies modulated differently between strains RH and ME49 (Fig. S1B and Table S1). We selected 220 targets regulated via translation and 30 nonregulated genes for validation using a custom-designed nCounter code set from NanoString Technologies (Table S2). Targets were selected based on biological functions of the encoded proteins that were of particular interest (e.g., cell death, metabolism, the immune response, and translation). In addition, expression levels (similar numbers of low, intermediate, and high levels of polysome-associated mRNAs) and proportions of the directionality of translational regulation (~1/3 up- and ~2/3 downregulated) were also considered selection criteria. Changes in translational efficiency as estimated by RNA-Seq and nCounter assays were highly correlated (Spearman rank correlation, ρ, values of 0.76 for RH versus the control, 0.76 for ME49 versus the control, and 0.56 for RH versus ME49) (Fig. S1C). Accordingly, mRNAs identified as translationally activated or repressed using RNA-Seq largely showed a consistent directionality of regulation. Thus, both *T. gondii* strains induce abundant and similar selective changes in the host cell translational efficiency.

***T. gondii* selectively reprograms translation of mRNAs encoding proteins involved in protein synthesis, cell activation, and cytoskeleton/cytoplasm organization.** To identify functional classes enriched for translationally regulated host mRNAs and to predict biological processes consequently affected during *T. gondii* infection, we used Ingenuity Pathway Analysis (IPA) (46). Within the molecular and cellular functions IPA classification, several functional networks were significantly enriched (FDR of <0.05) among proteins encoded by mRNAs whose translation was altered during *T. gondii* infection relative to the background (all mRNAs detected by RNA-Seq described above) (Fig. 2A; see also Table S3 in the supplemental material). The enriched categories include mRNAs involved in translation, the organization of the cytoskeleton and cytoplasm, cell activation, and cell movement. Globally, translational efficiencies of targets that belong to these categories displayed similar directionalities of regulation by RH and ME49 (Fig. 2B). Within the "translation" category, all mRNAs encoding ribosomal proteins were translationally activated. Conversely, targets grouped in the category "organization of the cytoplasm and cytoskeleton" were generally repressed. These transcripts encode proteins involved in membrane dynamics, microtubule-based movement, organelle formation and organization, and vesicular trafficking (e.g., dyneins *Dync1H1* and *Dync2H1*; kinesins *Kif11* and *Kif3A*; and myosins *Myh10*, *Myo6*, *Myo7A*, *Myo10*, and *Myo18A*). Within the category "activation of cells," translational efficiencies of some mRNAs related to cell movement and chemotaxis were activated (chemokines *Ccl5* and *Ccl9*), while others were repressed (chemokine receptors *Ccr2*, *Ccr5*, and *CxcCr1* and matrix metalloproteases *Mmp9* and *Mmp13*). Although not classified in this category by IPA, *Mmp8*, *Mmp11*, and *Mmp12* were also identified as translationally downregulated upon infection (Table S1). Notably, mRNAs encoding immune cell activators were largely repressed (CD molecules *Cd2*, *Cd93*, and *Cd180*; interleukin receptors *Il2Rb1*, *Il18Rap*, and *Il6Ra*; and integrins *Itgam* and *Itgav*). In stark contrast, transcripts involved in immune suppression and negative regulation of inflammation (e.g., *Cd200* and *Il1Ra*) were more efficiently translated in infected cells (Fig. 2B). Interestingly, the translational repression of transcripts promoting cell death was concomitant with the translational activation of antiapoptotic and cell cycle progression regulators. For instance, the levels of the negative regulator of cell differentiation *Notch2* and the proapoptotic transcription factor *Foxo3a* were decreased, whereas the levels of antiapoptotic and positive regulators of cell cycle progression and macrophage differentiation were enhanced (e.g., *Bcl2A1D* and *Hbegf*) (Fig. 2B). Consistent with this, other negative regulators of cell proliferation and differentiation (*Bcl6* and *Notch4*) were also translationally repressed (Table S1). Thus, *T. gondii* appears to selectively modulate the translational efficiencies of host mRNAs favoring the survival of infected cells while reorganizing the host cell architecture and preventing deleterious immune responses.

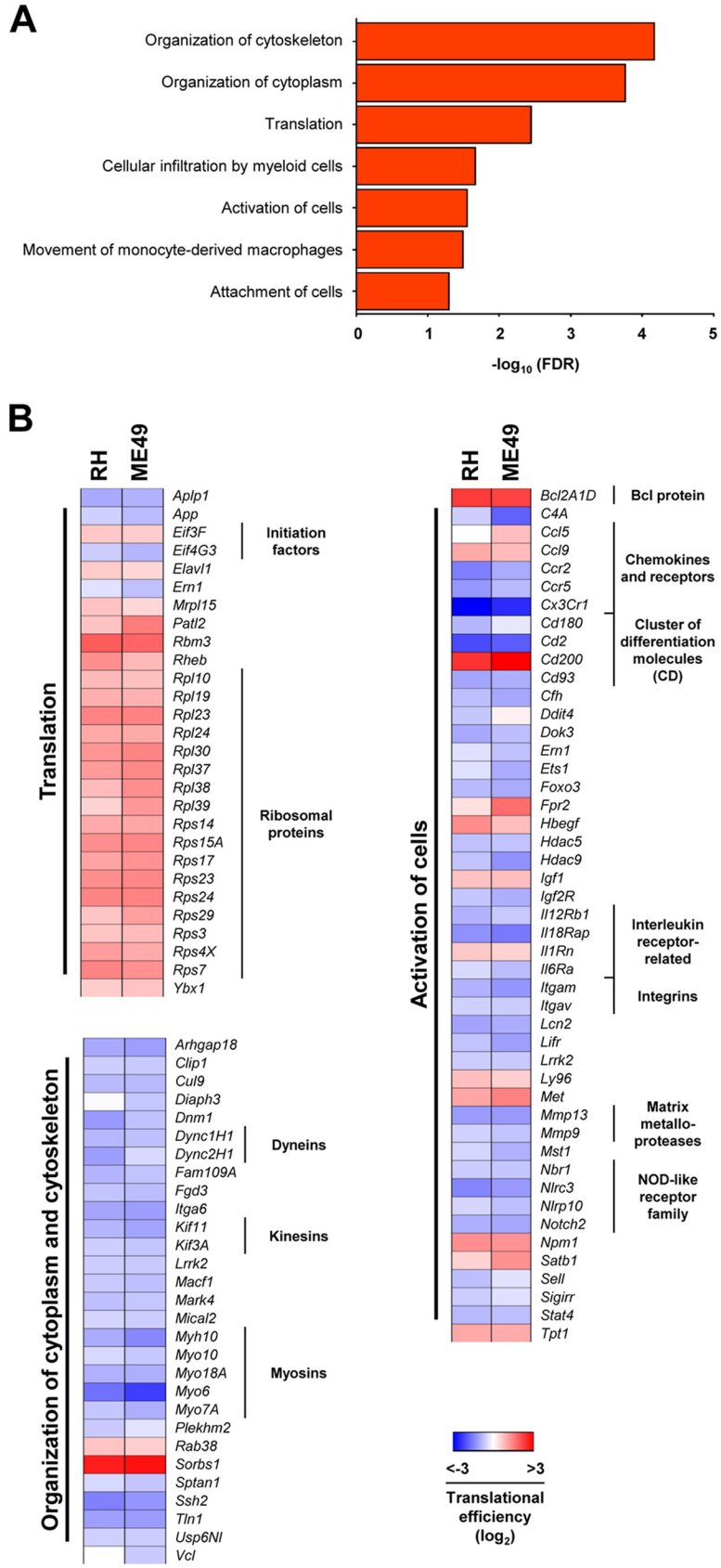

FIG 2 Enriched cell processes for translationally regulated host mRNAs upon *T. gondii* infection. IPA was performed on mRNAs translationally regulated by *T. gondii* infection. (A) FDR values ($-\log_{10}$) for select

(Continued on next page)

***T. gondii* infection selectively activates mTOR-sensitive translation.** We next assessed whether altered selective translation following parasite infection could be linked to distinct 5′ UTR features. To this end, we first calculated the 5′ UTR GC content and length of nonredundant mouse 5′ UTRs collected in the RefSeq database (47). While no significant differences in GC content were observed (see Fig. S2A in the supplemental material), mRNAs translationally activated upon parasite infection had significantly shorter 5′ UTRs than the background (all RefSeq mouse 5′ UTRs) (Fig. 3A). Second, we searched for sequence motifs using MEME (Multiple Em for Motif Elicitation) (48). This analysis identified a contiguous pyrimidine-rich (CU) motif ($E = 2.6 \times 10^{-18}$) within 223 out of the 322 mRNAs showing activated translation (Fig. 3B and Table S4) and a GC-rich stretch ($E = 2.1 \times 10^{-215}$) in 314 out of the 625 translationally suppressed transcripts (Fig. S2B and Table S4). Interestingly, the CU motif has some resemblance to the 5′ TOP motif CY_n ($n \geq 4$), where Y represents a pyrimidine nucleoside (49). TOP-containing mRNAs encode ribosomal proteins and factors for translation initiation and elongation (eIFs and eukaryotic elongation factors [eEFs]) whose translational efficiency is sensitive to mTOR activity (50–52). Indeed, translation of TOP mRNAs was selectively activated following infection with both parasite strains ($P < 0.001$ for RH and ME49 versus the control) (Fig. 3C and D and Table S5). In contrast, the translational efficiencies of internal ribosome entry site (IRES)-containing mRNAs were largely unaffected upon infection (Fig. 3D and Table S5). In addition to TOP mRNAs, transcripts with short 5′ UTRs whose translation is also mTOR-dependent but does not require a 5′ TOP motif, such as those encoding mitochondrion-related proteins (51), were translationally activated in infected cells (i.e., mRNAs related to mitochondrial translation, the electron transport chain, the mitochondrial respiratory chain, and the mitochondrial proton-transporting ATP synthase complex) (Fig. 3E and Table S5).

The data described above indicate that increased mTOR activity underlies a substantial proportion of parasite-induced changes in the translatome. To directly assess this, we used a previously reported translation signature (53), consisting of mRNAs whose translation efficiency is suppressed following mTOR inhibition (using PP242 in the breast carcinoma cell line MCF-7). Indeed, infection with either strain was associated with selectively activated translation of such mTOR-sensitive mRNAs ($P < 0.001$ for RH and ME49 versus the control) (Fig. 3F and Table S5). Altogether, these data suggest that *T. gondii* selectively augments mTOR-sensitive translation in BMDM.

***T. gondii* infection increases host mTORC1 activity in BMDM.** The translation of mRNAs whose translational efficiency parallels mTOR activity was enhanced in *T. gondii*-infected macrophages. Therefore, we next determined mTORC1 kinase activity by assessing the phosphorylation of its downstream targets, S6K1/S6K2 and 4E-BP1/4E-BP2. Of note, parasite extracts (i.e., devoid of any host cell ["*Tg* only"]) were probed in parallel to rule out the possibility that the observed changes in mTORC1 signaling were due to cross-reactivity of the antibodies against parasite proteins (Fig. 4A). Phosphorylation of S6K1 (T389) and levels of S6K2 were increased in BMDM infected with either the RH or ME49 strain (Fig. 4A). Accordingly, the phosphorylation of the downstream target of S6K1/S6K2, ribosomal protein S6 (RPS6) (S235, S236, S240, and S244), was augmented and required active invasion without noticeable bystander effects (see Fig. S3A in the supplemental material). Phosphorylation of RPS6 in infected cells was completely abrogated in S6K1$^{-/-}$/S6K2$^{-/-}$ BMDM, confirming that this cellular response is S6K1/S6K2 dependent (Fig. S3B). In addition, the hierarchical phosphorylation of 4E-BP1/4E-BP2 (i.e., T37/46, T70, and S65) was induced in *T. gondii*-infected BMDM with similar kinetics for the two strains (Fig. 4A). Hyperphosphorylation

FIG 2 Legend (Continued)
biologically relevant IPA categories that were significantly enriched in *T. gondii*-infected cells. (B) Heat maps showing translational efficiency changes for selected genes in enriched categories were generated by using Morpheus (Broad Institute [see https://software.broadinstitute.org/morpheus/index.html]). For panels A and B, analyses were carried out on data generated from three independent biological replicates.

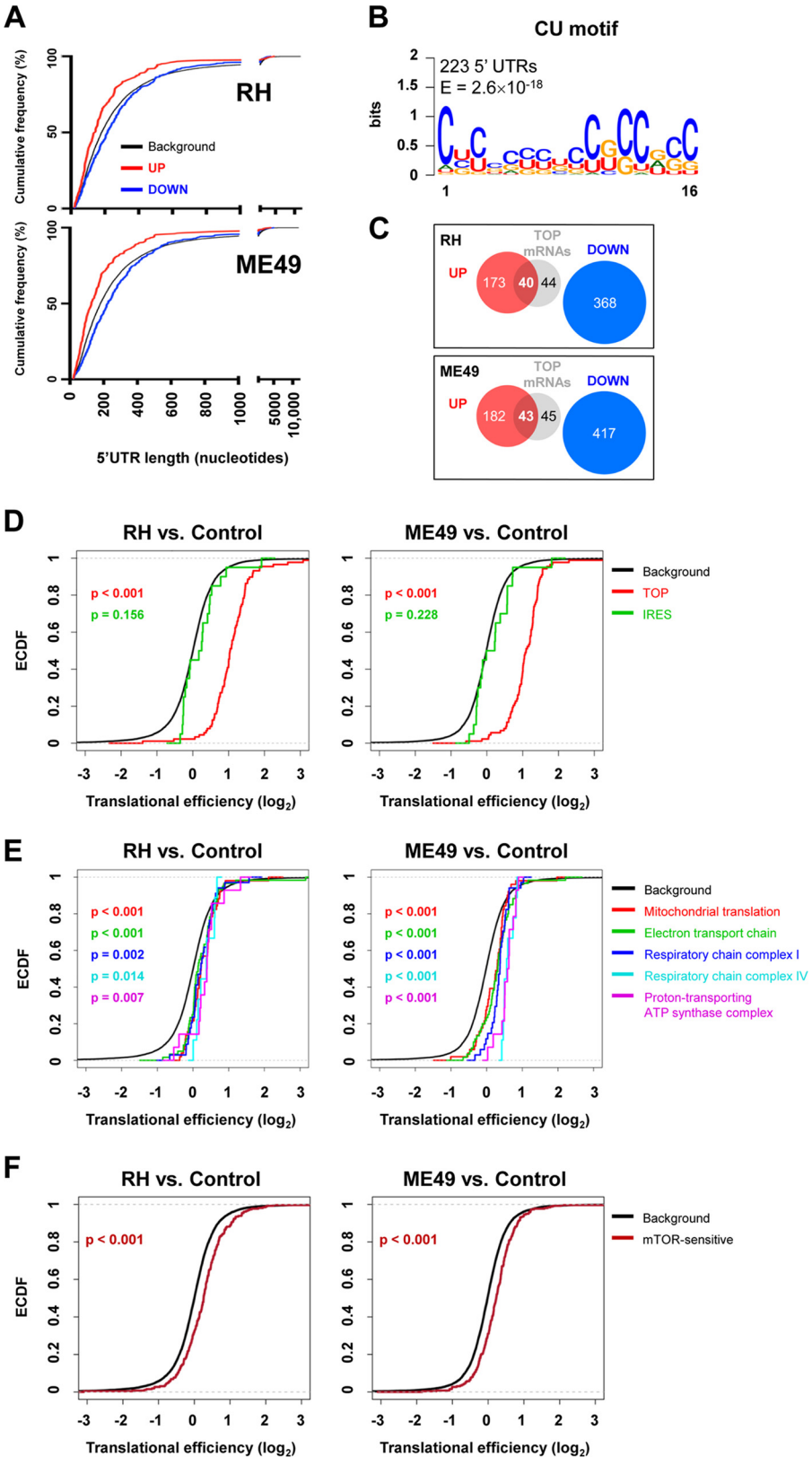

FIG 3 *T. gondii* infection selectively activates mTOR-sensitive translation. (A) Cumulative frequency distri butions of RefSeq 5′ UTR lengths across the mm10 genome (black), compared to those of the upregulated and downregulated sets in RH (top) and ME49 (bottom) infections. (B) Sequence logo of the MEME motif found in the upregulated 5′ UTR set. Nucleotide positions are indicated on the *x* axis. (C) Venn diagrams indicating the numbers of genes harboring a TOP motif present in the upregulated versus downregulated

(Continued on next page)

of 4E-BP1/4E-BP2 was also evident by a mobility shift on SDS-PAGE gels and increased amounts of the γ form compared to the α and β forms. The hyperphosphorylated forms of 4E-BP1/4E-BP2 have lower affinities for the mRNA 5′-m^{7}G cap-binding protein eIF4E (29). Consistently, m^{7}GTP pulldown assays revealed a reduced interaction between 4E-BP1/4E-BP2 and m^{7}GTP-bound eIF4E in *T. gondii*-infected BMDM (Fig. 4B and C). Treatment with Torin-1, an active-site TOR inhibitor (asTORi) (54), resulted in the complete dephosphorylation of 4E-BP1/4E-BP2 and strong binding to m^{7}GTP-bound eIF4E regardless of the infection status of the host cell (Fig. 4B). In summary, *T. gondii* activates mTORC1 signaling and promotes the dissociation of 4E-BP1/4E-BP2 from cap-bound eIF4E in BMDM.

Next, we aimed to elucidate upstream events activating mTORC1 during *T. gondii* infection. To this end, we assessed the contribution of AKT, which phosphorylates and inactivates the mTORC1 repressor TSC2 (55). Pretreatment with a pan-AKT inhibitor, MK-2206 (56), partially decreased the phosphorylation of RPS6 and 4E-BP1 (Fig. S3C). In light of these results, we monitored mTORC1 activity in *T. gondii*-infected BMDM deprived of L-leucine, an amino acid whose intracellular levels regulate mTORC1 in an AKT-independent fashion (57). Simultaneous pharmacological inhibition of AKT and L-leucine starvation abrogated RPS6 and 4E-BP1 phosphorylation in *T. gondii*-infected BMDM (Fig. S3C). Altogether, these data suggest that the activation of mTORC1 in *T. gondii*-infected BMDM relies on both AKT-dependent and -independent mechanisms.

Inhibition of mTOR reverses *T. gondii*-induced activation of host mRNA translation and dampens parasite replication. To further assess whether changes in translational efficiency observed in *T. gondii*-infected cells depend on mTOR, polysome tracings were generated from BMDM treated with rapamycin, an allosteric mTORC1 inhibitor, or Torin-1. Rapamycin induced similar shifts from heavy polysomes to monosomes in RH- and ME49-infected BMDM (48.3% and 37.2% reductions, respectively) (Fig. 5A and B). As expected, Torin-1 exerted a more dramatic effect than rapamycin (RH, 62.2%; ME49, 62.5%), owing to its greater potency (54). Of note, no differences in infection rates and no acute toxicity were observed for parasites exposed to the inhibitors (see Fig. S4 in the supplemental material). While rapamycin and Torin-1 abrogated the phosphorylation of S6K1 (T389) and its downstream target RPS6 (S235, S236, S240, and S244) in *T. gondii*-infected BMDM, only Torin-1 completely abolished 4E-BP1/4E-BP2 phosphorylation (as described previously [58]) (Fig. 5C). To evaluate whether chemical inhibition of mTOR is sufficient to reverse the translation program induced following parasite infection, we performed polysome profiling, quantified by nCounter assays (same targets as the ones described above) (Table S2), in *T. gondii*-infected and uninfected BMDM treated with rapamycin or Torin-1. We next assessed how fold changes in polysome-associated and cytosolic mRNA levels (for the subset of mRNAs translationally activated upon infection by either RH or ME49) were affected in cells treated with rapamycin or Torin-1. This approach revealed that chemical inhibition of mTOR is sufficient to largely reverse the effects on selective translation induced during parasite infection (Fig. 5D and Table S6).

As parasite infection appears to profoundly affect host cell properties essential for the synthesis of biomolecules and growth by perverting host mTOR-sensitive mRNA translation, we hypothesized that the upregulation of mTOR activity constitutes a

FIG 3 Legend (Continued)
gene sets. (D) Cumulative distribution of translational efficiencies of TOP mRNAs, IRES-containing mRNAs, and the background (all transcripts). (E) Cumulative distribution of translational efficiencies of mRNAs related to mitochondrial translation, the electron transport chain, mitochondrial respiratory chain complex I, mitochondrial respiratory chain complex IV, the proton-transporting ATP synthase complex, and the background (all transcripts). (F) Cumulative distribution of translational efficiencies of mRNAs whose translation was previously defined as depending on mTOR activity and the background (transcripts not belonging to the gene signature). For panels D to F, changes in translational efficiencies between RH-infected (left) or ME49-infected (right) BMDM and uninfected cells were evaluated. *P* values determined by a Wilcoxon test are indicated (tests consider genes belonging versus those not belonging to each group). ECDF, empirical cumulative distribution function. For panels A to F, data analyses were conducted on samples obtained from three independent biological replicates.

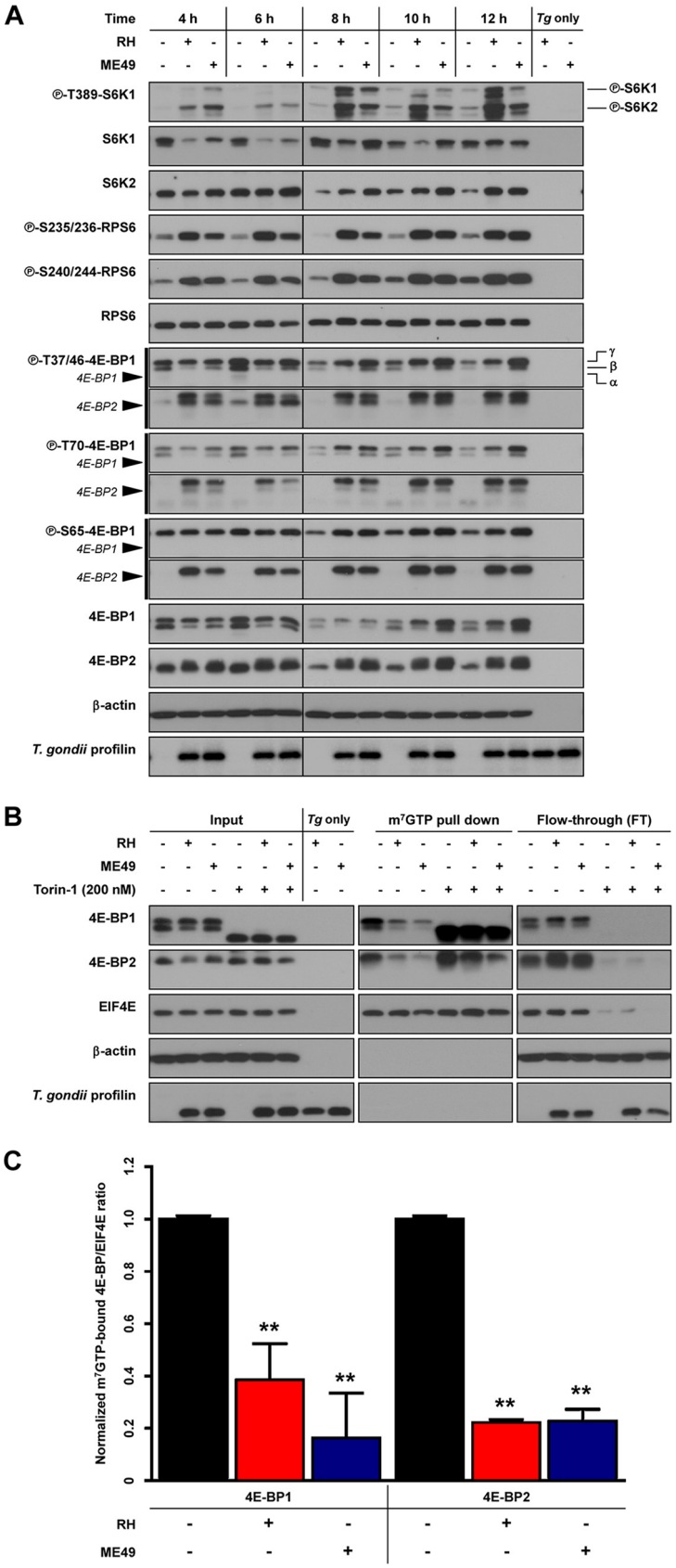

FIG 4 *T. gondii* augments mTORC1 activity and promotes 4E-BP1/4E-BP2 dissociation from cap-bound eIF4E in BMDM. (A) BMDM cultures were inoculated with either RH or ME49 *T. gondii* tachyzoites or left

(Continued on next page)

parasite survival strategy. To test this, BMDM were pretreated with either rapamycin or Torin-1 and infected with either RH or ME49 *T. gondii* tachyzoites. Parasites were allowed to egress and reinfect new host cells for 72 h, after which parasite numbers were evaluated by quantitative PCR (qPCR). Rapamycin treatment had a modest effect on parasite proliferation (12.8% and 19.5% reductions for RH and ME49, respectively), while Torin-1 caused a more pronounced reduction in replication (57.1% and 55.1%, respectively) than did dimethyl sulfoxide (DMSO) treatment (Fig. 5E). These data indicate that *T. gondii* relies on augmenting mTOR activity for unhindered replication.

DISCUSSION

Translational control of gene expression is a central mechanism of host defense (31, 32). As such, pathogens hijack the host translation machinery to survive (31, 32). Using transcriptome-wide polysome profiling, we demonstrate that the protozoan parasite *T. gondii* selectively augments mTOR-sensitive translation to favor host cell survival and parasite replication. Type I and II *T. gondii* strains regulate mTOR activity and mRNA translation in similar fashions, suggesting that this is a core process needed for parasite propagation that does not depend on strain-specific virulence factors. Further supporting the notion that regulation of mTOR-sensitive mRNA translation constitutes a parasite survival strategy, mTOR inactivation dampened *T. gondii* replication.

Our data on the activation of mTOR signaling are consistent with those of a recent analysis of the phosphoproteome of *T. gondii*-infected human foreskin fibroblasts (HFF) showing an enrichment of phosphorylated proteins both up- and downstream of mTOR, including RPS6 and 4E-BP1 (59). Interestingly, Wang and colleagues had previously reported that the phosphorylation of S6K1 following *T. gondii* infection was not consistently observed in different host cell lines (HFF, 3T3, and HeLa) (60–62). In some cases, no increased or prolonged phosphorylation of S6K1 was observed (60, 61), while in others, sustained and augmented phosphorylation was detected (62). To resolve the S6K-dependent phosphorylation of S6 in our experimental setting, we combined a chemical approach (i.e., mTOR inhibitors) and a genetic approach (i.e., BMDM derived from *s6k1/s6k2* double-knockout [DKO] mice) that confirmed the requirement for S6K1 and S6K2 activity for RPS6 phosphorylation in *T. gondii*-infected macrophages. Our results showing inducible and sustained phosphorylation of 4E-BP1 following infection are also in sharp contrast to those of Wang and colleagues, who reported the absence of this phenomenon in *T. gondii*-infected 3T3 and HeLa cells (60, 61). This discrepancy might be related to distinct signals triggered by *T. gondii* depending on the species and/or the type of host cell, which could result in the differential activation of mTOR effectors. Further characterization of mTOR outputs in immune and nonimmune cell populations will shed light on this matter. The mechanism by which *T. gondii* upregulates mTOR activity appears to be multifactorial, as indicated by the requirement for both AKT-mediated signaling and AKT-independent events, such as L-leucine availability. Amino acid abundance promotes Rag-dependent translocation and activation of mTORC1 at the lysosomal surface (63). Notably, mTOR associates with the parasitophorous vacuole (PV) in *T. gondii*-infected cells (60). Those observations, along with our

FIG 4 Legend (Continued)
uninfected for the indicated times. Phosphorylation and expression levels of indicated proteins were monitored by Western blotting. Total amounts of β-actin were used as a loading control, and an antibody against *T. gondii* profilin-like protein was employed to assess infection of BMDM cultures. Total protein extracts from extracellular tachyzoites (both the RH and ME49 strains) (*Tg* only) were used to control for any cross-reactivity of the antibodies against *T. gondii* proteins. (B) BMDM cultures were pretreated with 200 nM Torin-1 or an equal volume of DMSO (vehicle) for 2 h and then inoculated with either RH or ME49 *T. gondii* tachyzoites or left uninfected. Total protein extracts were collected at 8 h postinfection and prepared for m^{7}GTP pulldown assays. Levels of the indicated proteins in the input (15 μg), pulled-down material (20%), and flowthrough (FT) (15 μg) were determined by Western blotting. (C) Ratios of m^{7}GTP-bound 4E-BP/eIF4E were calculated based on densitometric measurements of the band intensities of 4E-BP1, 4E-BP2, and eIF4E and normalized to values for the uninfected BMDM control (means [SD]; $n = 3$ biological replicates). For panels A and B, data are representative of results from at least three independent biological replicates. **, $P < 0.01$.

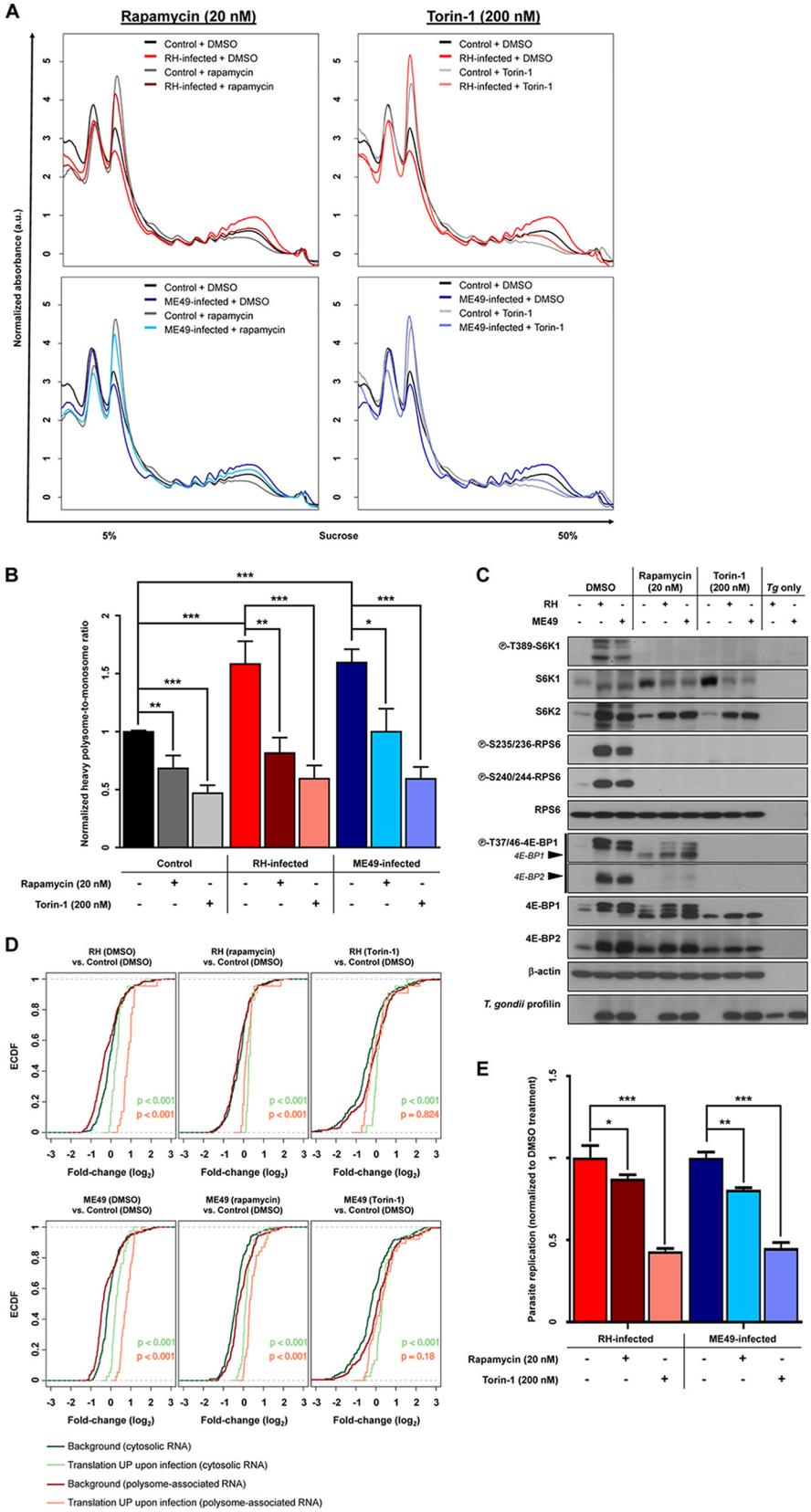

FIG 5 Inhibition of mTOR reverses *T. gondii*-induced activation of host mRNA translation and dampens parasite replication. BMDM cultures were pretreated with 20 nM rapamycin, 200 nM Torin-1, or an equal volume of DMSO (vehicle) for 2 h and then inoculated with either RH or ME49 *T. gondii* tachyzoites or left

(Continued on next page)

data, suggest that the PV surface offers a favorable site for mTORC1 activation during *T. gondii* infection.

Chemical inhibition of mTOR allowed us to confirm its requirement for selective translational activation in *T. gondii*-infected macrophages. Consistent with this, numerous mRNAs containing a 5′ TOP motif were present exclusively among translationally activated mRNAs, including those encoding ribosomal proteins. Interestingly, several of them play a role in cell cycle progression (e.g., RPS3, RPS7, RPS15a, RPL15, and RPL36a) and the regulation of apoptosis (e.g., RPS14, RPS29, and RPL7) (64). Moreover, *T. gondii* suppressed the translation of macrophage mRNAs encoding proapoptotic proteins, such as *Foxo3a*, while leading to the translational activation of prosurvival factors and cell cycle regulators (e.g., *Bcl2A1D*, *Cdk2*, *Hbegf*, and *Id2*). *T. gondii* has the ability to inhibit apoptosis and regulate the host cell cycle to promote infection (65–68). Moreover, mTOR activity is required for host cell cycle progression during *T. gondii* infection (60). In view of those studies and our present findings, *T. gondii* appears to regulate the translational efficiency of select mRNAs that favor the survival of the infected cell and ultimately enhance parasite replication.

Enrichment for transcripts encoding proteins related to cell activation and movement was mainly associated with translational repression by *T. gondii*. Strikingly, several of these factors are critical during toxoplasmosis. For instance, mice deficient in *Ccr2* fail to recruit $Gr1^+$ inflammatory monocytes to the intestine and are susceptible to oral challenge with *T. gondii* cysts (69). Similarly, genetic deletion of *Ccr5* increases susceptibility to toxoplasmosis, and signaling through this receptor is required for interleukin-12 (IL-12) production by dendritic cells in response to *T. gondii* (70). In stark contrast, *Cd200*, whose translational efficiency was activated in *T. gondii*-infected macrophages, has a detrimental effect during chronic toxoplasmosis. Indeed, CD200 expression downregulates microglial activation in the brain of *T. gondii*-infected mice. Accordingly, $Cd200^{-/-}$ mice display an efficient local antiparasitic response (71). Those studies, along with our data, indicate that selective translational control of immune-related genes by *T. gondii* contributes to its ability to subvert protective immune responses.

Numerous mRNAs pertaining to mitochondrial functions were translationally activated upon *T. gondii* infection, including mitoribosomal proteins, factors implicated in the electron transport chain, and ATP synthases. These data are consistent with the mTOR-sensitive translation of mRNAs encoding proteins related to mitochondrial biogenesis and functions (72, 73). With regard to *T. gondii*, it is well documented that the PV associates with the host mitochondria (74–76). Accumulating evidence indicates

FIG 5 Legend (Continued)
uninfected (control) for 8 h. (A) Polysome tracings representative of data from at least four independent biological replicates. a.u., arbitrary units. (B) Heavy polysome-to-monosome ratios normalized to values for DMSO-treated uninfected BMDM cultures (control) (means [SD]; $n = 4$ biological replicates). (C) A fraction of the cultures utilized for polysome tracings was used to collect total protein extracts. The phosphorylation status and expression levels of the indicated proteins were monitored by Western blotting. Data are representative of results from four separate experiments. (D) Transcripts showing activated translational efficiencies following parasite infection were selected, and their mTOR-sensitive translation was assessed by using polysome profiling coupled to nCounter assays (same treatments as for panel A). The cumulative distributions of $\log_2$ fold changes for these targets were compared to the background (all other nCounter-quantified mRNAs) in infected cells with or without rapamycin or Torin-1 treatment and compared to values for uninfected DMSO controls. Empirical cumulative distribution functions (ECDF) are shown for $\log_2$ fold changes for cytosolic mRNA and polysome-associated mRNA. UP, upregulated. *P* values for comparison of selected targets with their corresponding background, determined by Wilcoxon tests, are given. Data analyses were conducted on samples obtained from three independent biological replicates. (E) BMDM were pretreated with 20 nM rapamycin, 200 nM Torin-1, or an equal volume of DMSO (vehicle) for 2 h and then inoculated with either RH or ME49 *T. gondii* tachyzoites at a parasite-to-BMDM ratio of 1:20 for 72 h. Genomic DNA was extracted, and parasite replication was assessed by qPCR by amplification of the *T. gondii* B1 gene. C_T values were normalized to the value for mouse β-actin, and effects of the inhibitors on parasite replication were calculated by normalization to values obtained from cultures treated with DMSO for each strain. Values from one representative experiment of two independent trials are presented as means (SD); experiments on all samples were performed in technical triplicates. *, $P < 0.05$; **, $P < 0.01$; ***, $P < 0.001$.

that this association not only provides the parasite with nutrients, such as amino acids and glucose (77), but also leads to altered oxidative phosphorylation (OXPHOS) (78) and impacts innate immune responses (79). Moreover, the metabolism of intracellular *T. gondii* tachyzoites appears to rely on host-derived ATP (80), and parasite egress is particularly sensitive to host cell ATP levels (81). Therefore, it is plausible that the translational control of select host mRNAs by *T. gondii* contributes to the subversion of host mitochondrial functions, which in turn favors parasite metabolic activity and replication. Future studies should therefore aim to address these issues.

Several genes related to autophagy were identified in our study as translationally repressed in *T. gondii*-infected cells (e.g., *Atp13a2*, *Htr2b*, *Iigp1*, *Kdr*, *Lrrk2*, *Nbr1*, *Tecpr1*, *Tpcn1*, *Trim21*, and *Wdfy3*), while others were activated (e.g., *Hspa8* and *Mefv*). Interestingly, host autophagy appears to have a dual role during *T. gondii* infection since it provides macromolecules to replicating parasites (82) but also contributes to parasite clearance by stripping the PV membrane (83). TRIM20, encoded by the *MEFV* gene, is induced by gamma interferon (IFN-γ) and is involved in "precision autophagy," by specifically targeting the inflammasome components NLRP3, procaspase 1, and NLRP1 to limit excessive inflammation (84). Therefore, by favoring the translational efficiency of *MEFV*, it possible that the parasite aims at limiting inflammasome activation, a mechanism required for host resistance against *T. gondii* (85, 86). Translational repression of *Iigp1* and *Trim21* could also favor parasite persistence within the infected cell. IIGP1 (or Irga6) is targeted and inactivated by the parasite virulence factor kinase complex ROP5/ROP18/GRA7 (87) to prevent immune-related GTPase (IRG)-mediated destruction of the parasite (88, 89). Similarly, TRIM21 accumulates at the PV membrane following IFN-γ stimulation to restrict parasite replication and modulate inflammatory cytokine production in *T. gondii*-infected cells (90). Moreover, *Trim21*-deficient mice are more susceptible to toxoplasmosis and display higher parasite burdens and lower proinflammatory cytokine levels. Hence, it is tempting to suggest that modulation of translational efficiency of host mRNAs involved in autophagy constitutes an additional mechanism employed by *T. gondii* to promote infection.

In addition to the identification of pyrimidine-rich (CU) motifs in the 5′ UTR of mRNAs translationally activated upon *T. gondii* infection, 5′ UTR analysis indicated the presence of GC-rich stretches in ~50% of the mRNAs that are translationally repressed. Of interest, this feature was absent in the mRNAs whose translation was activated upon parasite infection. GC-rich motifs in the 5′ UTR are associated with the formation of secondary structures that limit mRNA translation efficiency (91, 92). Translational control is also achieved via *trans*-regulatory factors, such as RNA-binding proteins, microRNAs, and "specialized ribosomes" (93–95). A recent study by Fischer and colleagues reported that infection by *T. gondii* causes the formation of stress granules containing poly(A)-binding proteins (PABPs) in the nucleus of the host cell (96). PABPs regulate several steps in mRNA processing, such as export, degradation, stability, polyadenylation, and deadenylation (97, 98). Upon stress (e.g., UV irradiation or viral infection), mRNA can be stored in nuclear stress granules through interactions with PABPs leading to translational silencing (99). Further investigation is needed to define the role of PABPs in translational control during *T. gondii* infection. It is conceivable that numerous mechanisms act in concert during *T. gondii* infection to fine-tune selective host mRNA translation.

Collectively, this study defines the translational signature of macrophages infected by *T. gondii* and provides evidence that translational control constitutes a key mechanism of host cell subversion by the parasite. Further supporting a central role for posttranscriptional regulatory mechanisms of gene expression during toxoplasmosis, a lack of correlation between transcriptomic and proteomic data was reported for human fibroblasts infected by *T. gondii* (100). Thus, it is likely that by modulating translation efficiencies in different cell types, *T. gondii* promotes its survival and dissemination through the infected host. Future studies using *in vitro* and *in vivo* models of *T. gondii* infection will contribute to a better understanding of the impact and the mechanisms underlying the regulation of mRNA translation during toxoplasmosis.

MATERIALS AND METHODS

Reagents. Culture media and supplements were purchased from Wisent and Gibco; cycloheximide (CHX) was purchased from BioShop; CellTracker green CMFDA (5-chloromethylfluorescein diacetate) dye was purchased from Molecular Probes; RNasin was provided by Promega; rapamycin (sirolimus) was bought from LC Laboratories; Torin-1 and MK-2206 were purchased from Cayman; pyrimethamine was obtained from Tocris; XTT [2,3-bis-(2-methoxy-4-nitro-5-sulfophenyl)-2H-tetrazolium-5-carboxanilide] was ordered from Biotium; [5,6-^{3}H]uracil was purchased from Perkin-Elmer; cOmplete EDTA-free protease inhibitor and PhosSTOP phosphatase inhibitor tablets were purchased from Roche; DAPI (4′,6-diamidino-2-phenylindole dilactate) and CellTracker green (CMFDA) were acquired from Invitrogen; and primary and secondary antibodies for Western blotting and microscopy were purchased from Cell Signaling Technologies, Santa Cruz Biotechnology, R&D Systems, Sigma-Aldrich, BioLegend, and Invitrogen.

Parasite maintenance and harvest. *Toxoplasma gondii* tachyzoite cultures (RH and ME49 strains) were maintained by serial passages in Vero cells kindly provided by Angela Pearson (INRS-Institut Armand Frappier, Laval, QC, Canada), and cells were grown in Dulbecco's modified Eagle's medium (DMEM) supplemented with 5% heat-inactivated fetal bovine serum (FBS), 2 mM L-glutamate, 1 mM sodium pyruvate, 100 U/ml penicillin, and 100 μg/ml streptomycin and incubated at 37°C with 5% CO_2. For experimental infections, freshly egressed tachyzoites (RH and ME49 strains) were harvested from Vero cultures, pelleted by centrifugation (1,300 $\times$ *g* for 7 min at 4°C), resuspended in ice-cold phosphate-buffered saline (PBS) (pH 7.2 to 7.4), and passed through a syringe fitted with a 27-gauge needle. Large cellular debris and intact host cells were pelleted by low-speed centrifugation (200 $\times$ *g* for 3 min at 4°C), and the supernatant containing parasites was filtered with a 3-μm polycarbonate filter (Millipore). Tachyzoites were then washed twice in PBS and finally resuspended in the appropriate culture medium, according to the experiment.

Bone marrow-derived macrophage differentiation. Bone marrow-derived macrophages (BMDM) were obtained by differentiating precursor cells from murine bone marrow (101). Briefly, mice were euthanized by CO_2 asphyxiation, hind legs were collected in Hanks' balanced salt solution (HBSS) (100 U/ml penicillin, 100 μg/ml streptomycin, 4.2 mM sodium bicarbonate), and marrow was flushed out of bones. Red blood cells were lysed in ACK lysis buffer (150 mM NH_4Cl, 10 mM $KHCO_3$, 0.1 mM EDTA) for 7 min at room temperature (RT). Precursor cells were washed in HBSS, resuspended in BMDM culture medium (DMEM, 10% heat-inactivated FBS, 2 mM L-glutamate, 1 mM sodium pyruvate, 100 U/ml penicillin, 100 μg/ml streptomycin, 20 mM HEPES, 55 μM β-mercaptoethanol) supplemented with 15% L929 fibroblast-conditioned culture medium (LCCM), seeded into tissue culture-treated dishes, and incubated overnight at 37°C with 5% CO_2. The following day, cells that had not adhered were collected, resuspended in BMDM culture medium supplemented with 30% LCCM, and plated in regular petri dishes (i.e., 3 $\times$ 10^6 precursor cells per dish). Medium was changed 2 days later, and differentiated BMDM were collected 7 days after marrow extraction. Differentiation of precursor cells into macrophages was routinely assessed by monitoring CD11b and F4/80 coexpression by flow cytometry. Hind legs from *s6k1*$^{-/-}$/*s6k2*$^{-/-}$ C57BL/6 mice were kindly provided by Nahum Sonenberg (McGill University).

Ethics statement. Experiments were carried out under a protocol approved by the Comité Institutionnel de Protection des Animaux of the INRS-Institut Armand Frappier (CIPA number 1502-03). This protocol respects procedures on good animal practice provided by the Canadian Council on Animal Care.

Infection of BMDM. Macrophages were plated 1 day before infection with *T. gondii* in BMDM culture medium without LCCM and allowed to adhere overnight at 37°C with 5% CO_2. Cultures were serum starved for 2 h and treated with inhibitors, when applicable. BMDM were then inoculated with parasites (RH or ME49) or left uninfected in fresh medium with 1% FBS. Any remaining extracellular parasites were rinsed away with warm PBS (pH 7.2 to 7.4) 1 h following inoculation; fresh medium was added with inhibitors, when applicable; and cells were incubated until the end of the experiment. Unless specified otherwise, this procedure was carried out for all *in vitro* experiments.

Western blot analysis. Cultures were collected following infection and other treatments and lysed in ice-cold radioimmunoprecipitation assay (RIPA) lysis buffer (25 mM Tris [pH 7.6], 150 mM NaCl, 1% Triton X-100, 0.5% sodium deoxycholate, 0.1% SDS) supplemented with phosphatase and EDTA-free protease inhibitor cocktails (Roche, Basel, Switzerland). Insoluble material was removed by centrifugation (20,000 $\times$ *g* for 15 min at 4°C), and the protein concentration in the supernatant was measured by the bicinchoninic acid (BCA) assay, according to the manufacturer's specifications. About 20 μg of the protein sample was mixed with Laemmli loading buffer and subjected to SDS-PAGE, and the resolved proteins were transferred onto polyvinylidene difluoride (PVDF) membranes. Membranes were blocked for 1 h at RT in Tris-buffered saline (TBS)–0.05% Tween 20 plus 5% skim milk and then probed with the following primary antibodies: anti-4E-BP1, anti-phospho-4E-BP1 (T37/46), anti-phospho-4E-BP1 (T70), anti-phospho-4E-BP1 (S65), anti-4E-BP2, anti-phospho-RPS6 (S235/236), anti-phospho-RPS6 (S240/244), anti-phospho-S6K1, anti-S6K2, anti-AKT, anti-phospho-AKT (T308), anti-phospho-AKT (S473), and β-actin were obtained from Cell Signaling Technologies; anti-RPS6 and anti-S6K1 were purchased from Santa Cruz Biotechnology; anti-eIF4E was purchased from BD Biosciences; and anti-*T. gondii* profilin-like protein was purchased from R&D Systems. Membranes were then probed with either goat anti-rabbit, goat anti-mouse (Sigma-Aldrich), or rabbit anti-goat (R&D Systems) IgG horseradish peroxidase (HRP)-linked antibodies. Subsequently, proteins were visualized by using the Clarity ECL Western blotting substrate (Bio-Rad) and exposing the membranes to autoradiography film (Denville Scientific, Holliston, MA) or a chemiluminescence imager (Bio-Rad).

m^{7}GTP-agarose pulldown assay. BMDM cultures were plated in 10-cm-diameter plates in complete medium and allowed to adhere overnight at 37°C with 5% CO_2. Cultures were serum starved for 2 h in the presence of DMSO (vehicle), 20 nM rapamycin, or 200 nM Torin-1 and then inoculated with *T. gondii*

tachyzoites (RH and ME49 strains) at a multiplicity of infection (MOI) of 6:1 or left uninfected in fresh medium with 1% heat-inactivated FBS. Any remaining extracellular parasites were rinsed away with warm PBS (pH 7.2 to 7.4) 1 h following inoculation, fresh medium was added, and cells were incubated for an additional 7 h. Cultures were washed with ice-cold PBS, gently scraped, and pelleted by centrifugation (200 × *g* for 10 min at 4°C). Cells were lysed in ice-cold buffer A (lysis buffer) (50 mM morpholinepropanesulfonic acid [MOPS] [pH 7.4], 100 mM NaCl, 2 mM EDTA, 2 mM EGTA, 1% IGEPAL CA-630, 1% sodium deoxycholate, 7 mM β-mercaptoethanol) supplemented with phosphatase and EDTA-free protease inhibitor cocktails (Roche). Samples were incubated for 15 min on ice and regularly mixed gently, and the crude lysates were cleared by centrifugation (16,000 × *g* for 10 min at 4°C). The supernatant was transferred to new tubes, and the protein concentration was measured by the Bradford assay (Bio-Rad), according to the manufacturer's specifications. About 0.5 to 0.75 mg of proteins of each sample was mixed with a 50% slurry of 2′/3′-ethylenediamine-m^{7}GTP immobilized on agarose beads (Jena Bioscience) and diluted up to 1 ml with buffer B (wash buffer) (50 mM MOPS [pH 7.4], 100 mM NaCl, 0.5 mM EDTA, 0.5 mM EGTA, 7 mM β-mercaptoethanol, 0.1 mM GTP) supplemented with phosphatase and EDTA-free protease inhibitor cocktails (Roche). Samples were mixed for 1 h at 4°C with end-over-end (EOE) rotation. Beads were pelleted by centrifugation (500 × *g* for 1 min at 4°C). The supernatants (i.e., flowthrough [FT]) were kept, while the beads were washed twice in buffer B and finally resuspended in Laemmli loading buffer for further analysis by Western blotting.

Polysome-tracing analysis. BMDM cultures were plated in 15-cm-diameter plates overnight; serum starved for 2 h in the presence or absence of the vehicle (DMSO), 20 nM rapamycin, or 200 nM Torin-1; and then inoculated with *T. gondii* tachyzoites (RH and ME49 strains) at an MOI of 3:1 or left uninfected in fresh medium with 1% heat-inactivated FBS. After 8 h of infection, CHX was added to cultures to a final concentration of 100 μg/ml, and plates were incubated for 5 min at 37°C with 5% CO_2. Cells were then rinsed with cold PBS containing 100 μg/ml CHX, scraped, and pelleted by centrifugation (200 × *g* for 10 min at 4°C). Pellets were lysed in hypotonic lysis buffer (5 mM Tris [pH 7.5], 2.5 mM $MgCl_2$, 1.5 mM KCl, 2 mM dithiothreitol [DTT], 0.5% Triton X-100, 0.5% sodium deoxycholate, 100 μg/ml CHX, and 200 U RNasin RNase inhibitor [Promega, Madison, WI]), and lysates were cleared by centrifugation (20,000 × *g* for 2 min at 4°C). Lysates were loaded onto 5 to 50% sucrose density gradients (20 mM HEPES [pH 7.6], 100 mM KCl, 5 mM $MgCl_2$, 100 μg/ml CHX, and 200 U RNasin) and centrifuged in a Beckman SW41 rotor at 36,000 rpm for 2 h at 4°C. Gradients were fractionated and collected (30 s and 500 μl per fraction), and the absorbance at 254 nm was recorded continuously by using a Brandel BR-188 density gradient fractionation system.

Purification of RNA. Efficiently translated mRNA (associated with ≥3 ribosomes) and the input material (total cytoplasmic mRNA) were extracted with TRIzol (Invitrogen) and chloroform, followed by isopropanol precipitation. In brief, polysome fractions and input material were diluted up to 1 ml with RNase-free H_2O, and 500 μl of TRIzol and 150 μl of chloroform were then added. Samples were vortexed vigorously for 5 s, incubated for 3 min at RT, and centrifuged (18,000 × *g* for 15 min at 4°C). The aqueous phase of each sample was mixed with an equal volume (~750 μl) of ice-cold isopropanol and 1 μl of GlycoBlue (Thermo Fisher), and the RNA was then precipitated overnight at −20°C and pelleted by centrifugation (18,000 × *g* for 10 min at 4°C). The RNA pellet was washed twice with 500 μl of 75% ice-cold ethanol. Samples were air dried and resuspended in RNase-free H_2O, and polysome fractions from the corresponding treatment were pooled. RNA was further cleaned by using an RNeasy MinElute cleanup kit (Qiagen), according to the manufacturer's specifications. Finally, the approximate concentration, purity, and integrity of the purified RNA were assessed spectrophotometrically by using a NanoDrop 1000 instrument (Thermo Fisher) and a Bioanalyzer 2100 instrument with a eukaryote total RNA nanochip (Agilent Technologies). Samples were aliquoted and stored at −80°C until further analyses.

RNA-Seq data processing. Library preparation and sequencing were carried out at SciLifeLab (Stockholm, Sweden). RNA-Seq libraries were generated by using the strand-specific TruSeq protocol and sequenced by using an Illumina HiSeq2500 instrument with a single-end 51-base sequencing setup for both total cytosolic and polysome-associated mRNAs (mRNAs associated with >3 ribosomes) from three independent biological replicates. RNA-Seq reads from infected samples were first aligned to *T. gondii* reference genomes of GT1 (type I) and ME49 (type II) (the genome of the RH strain is not completely annotated, but it was estimated that among *T. gondii* RH gene families, 97.8% have orthologs in the GT1 strain [102]). Reads from infected samples that did not map to the *T. gondii* genomes as well as all reads from uninfected samples were aligned to the mouse genome mm10. HISAT2 was used for all alignments, with default settings (103). Alignments to *T. gondii* and *Mus musculus* resulted in 4.4% and 93.7% mappings on average, respectively. Gene expression was quantified by using the RPKMforgenes.py script (http://sandberg.cmb.ki.se/media/data/rnaseq/rpkmforgenes.py) (104) with options -fulltranscript -readcount -onlycoding, from which raw per-gene RNA-Seq counts were obtained (version last modified 2 July 2014). Annotation of genes was done by using RefSeq. Genes that had zero counts in all samples were removed. One replicate from the uninfected control condition was excluded from downstream analysis based on outlier behavior in principal-component analyses.

RNA-Seq analysis of the empirical data set using ANOTA. The limma::voom R function was used to compute $\log_2$ counts per million (105). To identify changes in translational efficiency leading to altered protein levels, ANOTA (45, 106) was used with the following parameters: minimum slope (minSlope) of −0.5 and maximum slope (maxSlope) of 1.5. Replicate was included as a batch effect in the models. The following criteria were considered for significant changes in translational efficiency: a false discovery rate (FDR) of <0.25, a translational efficiency (*apvEff*) of $>\log_2(1.5)$, a log ratio of polysome-associated mRNA data to cytosolic mRNA data (deltaPT) of $>\log_2(1.25)$, and a polysome-associated mRNA log fold change (deltaP) of $>\log_2(1.5)$. Genes that overlap, resulting in RNA sequencing reads that cannot be associated with only one gene, were excluded from downstream analyses. Similar FDR and fold change thresholds

were used when selecting differential expression of polysome-associated mRNAs. For further analysis, we used a previously reported list of TOP- and IRES-containing mRNAs (107), mitochondrion-related function genes included in the Gene Ontology (GO) (2015) terms indicated in Table S5 in the supplemental material, and a signature for mTOR-sensitive translation (53); gene symbols were converted from human to mouse and are listed in Table S5. The difference in $\log_2$ fold changes of translational efficiencies between the signatures and the background was assessed by using Wilcoxon-Mann-Whitney tests.

nCounter analysis. For nCounter analysis (NanoString Technologies), a subset of 250 genes was selected according to RNA-Seq data. Sequences for the probes in the custom-designed nCounter code set are listed in Table S2 in the supplemental material. Infected and uninfected cells were treated with rapamycin or Torin-1, followed by the isolation of efficiently translated mRNA and cytosolic mRNA from three independent biological replicates (as described above). The positive spike-in RNA hybridization controls for each lane were used to normalize NanoString counts as implemented in the posCtrlNorm function of the Bioconductor package NanoStringQCPro (108) (with parameter summaryFunction = "sum"). Targets with fewer than half of the samples above the background level (7 [$\log_2$ scale]) were excluded. The quality of the normalization was assessed by using 30 nonregulated genes selected from the RNA-Seq data analysis to verify that their expression levels remained stable in the DMSO samples. Spearman rank correlation coefficients were calculated between fold changes obtained from the RNA-Seq data and those obtained from the nCounter data. Analysis of translational control was performed with ANOTA to select targets that were translationally upregulated upon infection with each *T. gondii* strain. Genes with an FDR of <0.25 were considered significant, and the following parameters were used: minSlope of -1, maxSlope of 2, and selDeltaPT of $\log_2(1.2)$. For these targets, empirical cumulative distribution function (ECDF) curves were used to visualize the distribution of their $\log_2$ fold changes (for both cytosolic and polysome-associated mRNAs) upon treatment with rapamycin or Torin-1. Distribution differences were evaluated by using Wilcoxon-Mann-Whitney tests.

Functional classification of gene lists. Enrichment of translationally regulated genes in specific functional networks was determined by using Ingenuity Pathway Analysis (IPA; Qiagen) by comparing ANOTA-regulated gene sets against the entire sequenced data sets (46). Within the IPA application, statistical significance was calculated by using a right-tailed Fisher exact test, and *P* values were adjusted for multiple-hypothesis testing by using the Benjamini-Hochberg method to arrive at a FDR.

RNA sequence motif analyses. For 5′ UTR sequence analysis, nonredundant RefSeq 5′ UTRs were retrieved from genome build mm10 using the UCSC table browser (https://genome.ucsc.edu/cgi-bin/hgTables). The length and GC content of the UTRs were computed by using a custom script. To minimize the bias associated with analyzing GC contents and sequence motifs of very short sequences, 5′ UTRs of <20 nucleotides were omitted from further analyses. Novel RNA sequence motifs were detected in the 5′ UTRs by using MEME (Multiple Em for Motif Elicitation) (48). To accurately estimate the probability of a candidate motif appearing by chance (E value) and to improve the sensitivity of the motif search, a custom background model was employed. Briefly, the "fasta-get-markov" utility included in the program was used to compute a background Markov model of order 1 using all RefSeq mouse 5′ UTRs. Sequence logos were generated by using the ggseqLogo package in R. Cap analysis of gene expression (CAGE)-Seq data were retrieved from FANTOM5 (http://fantom.gsc.riken.jp/5/), and sequences were mapped to the mm9 build by using the UCSC genome browser.

XTT and [5,6-^{3}H]uracil incorporation viability assays. To test for acute toxicity of the inhibitors against extracellular tachyzoites, parasite viability was measured by using the tetrazolium reduction-based XTT assay (109). Briefly, freshly egressed tachyzoites (RH and ME49 strains) were resuspended in culture medium (without FBS) and transferred to 96-well plates (2×10^6 tachyzoites per well). Parasites were treated with 20 nM rapamycin, 200 nM Torin-1, or an equal volume of the vehicle (DMSO) and incubated for 2 h at 37°C with 5% CO_2. As a negative control, heat-killed (HK) parasites incubated at 56°C for 10 min were included in the assay. Next, the XTT reagents were prepared according to the manufacturer's specifications (Biotium) and added to the parasites. Tachyzoite cultures were incubated for 20 h. Absorbance was measured by using a Multiskan GO 1510 plate reader (Thermo Fisher) at 470 nm, from which the absorbance at 660 nm was subtracted.

To test for acute toxicity of the inhibitors on intracellular tachyzoites, the incorporation of 5,6-^{3}H-radiolabeled uracil by the parasite was measured as an assessment of viability (110). Briefly, BMDM were plated in 24-well plates overnight; serum starved for 2 h; treated with either 20 nM rapamycin, 200 nM Torin-1, or an equal volume of the vehicle (DMSO); and inoculated with *T. gondii* tachyzoites (RH and ME49 strains) at an MOI of 3:1 in fresh medium with 1% heat-inactivated dialyzed FBS. Cultures were incubated overnight, 5 μCi of [5,6-^{3}H]uracil (Perkin-Elmer) was then added to each well, and cultures were incubated for another 2 h at 37°C with 5% CO_2. Plates were chilled at -20°C for 2 min, an equal volume of ice-cold 0.6 N trichloroacetic acid (TCA) was added to each well, and cells were fixed on ice for 1 h. Wells were rinsed with PBS and then with deionized H_2O. Plates were air dried, and the precipitated material was resolubilized in 500 μl of 0.1 N NaOH for 1 h. Half of the material was thoroughly mixed with an equal volume of OptiPhase Supermix scintillation cocktail (Perkin-Elmer), and radioactivity was measured (counts per minute) with a MicroBeta TriLux scintillation counter (Perkin-Elmer). Uninfected cells were included to measure the background incorporation of uracil by host cells, and treatment with 10 μM pyrimethamine was included as a positive control for chemical toxicity against *T. gondii* parasites.

Immunofluorescence microscopy. BMDM were seeded onto glass coverslips in 24-well plates overnight, serum starved for 2 h, and then inoculated with *T. gondii* tachyzoites (RH and ME49 strains), previously stained with 20 μM CellTracker green CMFDA dye (Molecular Probes) for 20 min, at an MOI of 3:1 or left uninfected. After 8 h of infection, cells were rinsed with PBS three times and then fixed with 3.7% paraformaldehyde (PFA) (in PBS) for 15 min at RT. Cell membranes were permeabilized with 0.2%

Triton X-100 (in PBS) for 5 min at RT. Fc receptors and nonspecific binding sites were blocked by incubating samples with 5 μg/ml anti-CD16/32 (BioLegend) diluted in PBS supplemented with 10 mg/ml bovine serum albumin (BSA). Primary antibody against phospho-RPS6 (S240/244) (Cell Signaling Technologies) was diluted in PBS with 10 mg/ml BSA and incubated with samples for 1 h at RT. A goat anti-rabbit IgG(H+L) secondary antibody conjugated to Alexa Fluor 594 (Invitrogen) was incubated with the samples for 1 h at RT. Nuclei were stained with 300 nM DAPI (Invitrogen) for 5 min at RT. Coverslips were mounted onto slides with Fluoromount G (Southern Biotech). Samples were visualized by using a Leica microscope, and image processing was performed with Fiji (111).

Measurement of parasite replication by qPCR. Parasite replication *in vitro* was assessed by extracting genomic DNA (gDNA), followed by measuring the amplification of the *T. gondii* B1 gene by qPCR, as described previously (101). Briefly, BMDM cultures were plated in 12-well plates overnight; serum starved for 2 h in the presence of DMSO (vehicle), 20 nM rapamycin, or 200 nM Torin-1; and then inoculated with *T. gondii* tachyzoites (RH and ME49 strains) at an MOI of 1:20. Parasites were allowed to replicate, egress, and reinfect cells for 72 h. Culture supernatants were collected (for extracellular parasites), while the remaining adherent cells (containing intracellular parasites) were detached by adding ice-cold PBS with 5 mM EDTA for 15 min at 4°C, followed by vigorous pipetting, and then pooled into culture supernatants. Tachyzoites and host cells were pelleted by centrifugation (16,000 $\times$ *g* for 10 min at 4°C) and then resuspended in 200 μl PBS. gDNA was extracted by using a Roche High Pure PCR template preparation kit, according to the manufacturer's specifications. To measure parasite replication, the 35-fold repetitive *T. gondii* B1 gene was amplified by qPCR using the PowerUP SYBR green PCR master mix (Applied Biosystems) with the $MgCl_2$ concentration adjusted to 3.5 μM, 10 ng of template gDNA, and 0.5 μM forward primer (5′-TCCCCTCTGCTGGCGAAAAGT-3′) and reverse primer (5′-AGCGTT CGTGGTCAACTATCGATTG-3′) (Integrated DNA Technologies) in a 20-μl reaction mixture volume. The reaction was carried out in a QuantStudio 3 real-time PCR system (Applied Biosciences) with the following program: 10 min of initial denaturation at 95°C, followed by 45 cycles of 15 s of denaturation at 95°C, 30 s of annealing at 58°C, and 30 s of extension at 72°C. Cycle threshold (C_T) values were normalized by using mouse β-actin gene primers (0.2 μM forward primer 5′-CACCCACACTGTGCCCATC TACGA-3′ and reverse primer 5′-CAGCGGAACCGCTCATTGCCAATGG-3′), and the $MgCl_2$ concentration was adjusted to 2.5 μM. Analysis was carried out by relative quantification using the comparative C_T ($2^{-\Delta\Delta CT}$) method (112). The effect of the inhibitors on replication was calculated by normalization to values obtained from parasite cultures treated with DMSO. Values are presented as means (SD); experiments on all samples were performed in triplicates.

Statistical analysis. Where applicable, data are presented as means (SD). Statistical significance was determined by using one-way analysis of variance (ANOVA) followed by a Tukey *post hoc* test; calculations were performed by using Prism software (GraphPad, La Jolla, CA). Differences were considered significant when *P* values were <0.05, <0.01, or <0.001.

SUPPLEMENTAL MATERIAL

Supplemental material for this article may be found at https://doi.org/10.1128/IAI.00244-18.

SUPPLEMENTAL FILE 1, PDF file, 0.6 MB.
SUPPLEMENTAL FILE 2, PDF file, 0.3 MB.
SUPPLEMENTAL FILE 3, PDF file, 1.2 MB.
SUPPLEMENTAL FILE 4, PDF file, 0.6 MB.
SUPPLEMENTAL FILE 5, XLSX file, 0.1 MB.
SUPPLEMENTAL FILE 6, XLSX file, 0.1 MB.
SUPPLEMENTAL FILE 7, XLSX file, 0.1 MB.
SUPPLEMENTAL FILE 8, XLSX file, 0.1 MB.
SUPPLEMENTAL FILE 9, XLSX file, 0.1 MB.
SUPPLEMENTAL FILE 10, XLSX file, 0.1 MB.

ACKNOWLEDGMENTS

We are grateful to Nahum Sonenberg for providing bone marrow from C57BL/6 *s6k1*$^{-/-}$ *s6k2*$^{-/-}$ mice (McGill University, Montreal, QC, Canada). We thank Medhi Jafarnejad (McGill University) for technical advice. We are thankful to Annie Sylvestre and Annik Lafrance for invaluable technical assistance. We acknowledge support from the Science for Life Laboratory, the National Genomics Infrastructure (NGI), and Uppmax for providing assistance in massive parallel sequencing and computational infrastructure.

This work was supported by a Basil O'Connor starter scholar research award (5-FY14-78) and a research grant (6-FY16-151) from The March of Dimes Foundation to M.J. The Centre for Host-Parasite Interactions is supported by a Subvention de Regroupement Stratégique from the Fonds de Recherche du Québec en Nature et Technologies (FRQ-NT). M.J. is a recipient of a Bourse de Chercheur-Boursier Junior 1

from the Fonds de Recherche du Québec en Santé (FRQ-S) and a Subvention d'Établissement de Jeune Chercheur from the FRQ-S. V.C. is supported by a Ph.D. scholarship from the Fondation Universitaire Armand Frappier. Research in the laboratory of O.L. is supported by grants from the Swedish Research Council and the Wallenberg Academy Fellows program. The funders had no role in the study design, data collection and analysis, decision to publish, or preparation of the manuscript.

REFERENCES

1. Dubey JP. 2004. Toxoplasmosis—a waterborne zoonosis. Vet Parasitol 126:57–72. https://doi.org/10.1016/j.vetpar.2004.09.005.
2. Frenkel JK, Dubey JP, Miller NL. 1970. Toxoplasma gondii in cats: fecal stages identified as coccidian oocysts. Science 167:893–896. https://doi.org/10.1126/science.167.3919.893.
3. Dubey JP, Miller NL, Frenkel JK. 1970. The *Toxoplasma gondii* oocyst from cat feces. J Exp Med 132:636–662. https://doi.org/10.1084/jem.132.4.636.
4. Luft BJ, Remington JS. 1992. Toxoplasmic encephalitis in AIDS. Clin Infect Dis 15:211–222. https://doi.org/10.1093/clinids/15.2.211.
5. Montoya JG, Remington JS. 2008. Management of *Toxoplasma gondii* infection during pregnancy. Clin Infect Dis 47:554–566. https://doi.org/10.1086/590149.
6. Laliberte J, Carruthers VB. 2008. Host cell manipulation by the human pathogen *Toxoplasma gondii*. Cell Mol Life Sci 65:1900–1915. https://doi.org/10.1007/s00018-008-7556-x.
7. Hakimi MA, Olias P, Sibley LD. 2017. *Toxoplasma* effectors targeting host signaling and transcription. Clin Microbiol Rev 30:615–645. https://doi.org/10.1128/CMR.00005-17.
8. Hunter CA, Sibley LD. 2012. Modulation of innate immunity by *Toxoplasma gondii* virulence effectors. Nat Rev Microbiol 10:766–778. https://doi.org/10.1038/nrmicro2858.
9. Hakimi MA, Bougdour A. 2015. *Toxoplasma*'s ways of manipulating the host transcriptome via secreted effectors. Curr Opin Microbiol 26:24–31. https://doi.org/10.1016/j.mib.2015.04.003.
10. Gebauer F, Hentze MW. 2004. Molecular mechanisms of translational control. Nat Rev Mol Cell Biol 5:827–835. https://doi.org/10.1038/nrm1488.
11. Sonenberg N, Hinnebusch AG. 2009. Regulation of translation initiation in eukaryotes: mechanisms and biological targets. Cell 136:731–745. https://doi.org/10.1016/j.cell.2009.01.042.
12. Schneider RJ, Sonenberg N. 2007. Translational control in cancer development and progression, p 401–431. *In* Mathews MB, Sonenberg N, Hershey JW (ed), Translational control in biology and medicine. Cold Spring Harbor Laboratory Press, Cold Spring Harbor, NY.
13. Lasko P. 2012. mRNA localization and translational control in *Drosophila* oogenesis. Cold Spring Harb Perspect Biol 4:a012294. https://doi.org/10.1101/cshperspect.a012294.
14. Hershey JW, Sonenberg N, Mathews MB. 2012. Principles of translational control: an overview. Cold Spring Harb Perspect Biol 4:a011528. https://doi.org/10.1101/cshperspect.a011528.
15. Silvera D, Formenti SC, Schneider RJ. 2010. Translational control in cancer. Nat Rev Cancer 10:254–266. https://doi.org/10.1038/nrc2824.
16. Ruggero D. 2013. Translational control in cancer etiology. Cold Spring Harb Perspect Biol 5:a012336. https://doi.org/10.1101/cshperspect.a012336.
17. Ezegbunam W, Foronjy R. 2018. Posttranscriptional control of airway inflammation. Wiley Interdiscip Rev RNA 9:e1455. https://doi.org/10.1002/wrna.1455.
18. Parker MW, Rossi D, Peterson M, Smith K, Sikstrom K, White ES, Connett JE, Henke CA, Larsson O, Bitterman PB. 2014. Fibrotic extracellular matrix activates a profibrotic positive feedback loop. J Clin Invest 124:1622–1635. https://doi.org/10.1172/JCI71386.
19. Roffe M, Beraldo FH, Bester R, Nunziante M, Bach C, Mancini G, Gilch S, Vorberg I, Castilho BA, Martins VR, Hajj GN. 2010. Prion protein interaction with stress-inducible protein 1 enhances neuronal protein synthesis via mTOR. Proc Natl Acad Sci U S A 107:13147–13152. https://doi.org/10.1073/pnas.1000784107.
20. Ma T, Trinh MA, Wexler AJ, Bourbon C, Gatti E, Pierre P, Cavener DR, Klann E. 2013. Suppression of eIF2alpha kinases alleviates Alzheimer's disease-related plasticity and memory deficits. Nat Neurosci 16:1299–1305. https://doi.org/10.1038/nn.3486.
21. Moreno JA, Radford H, Peretti D, Steinert JR, Verity N, Martin MG, Halliday M, Morgan J, Dinsdale D, Ortori CA, Barrett DA, Tsaytler P, Bertolotti A, Willis AE, Bushell M, Mallucci GR. 2012. Sustained translational repression by eIF2alpha-P mediates prion neurodegeneration. Nature 485:507–511. https://doi.org/10.1038/nature11058.
22. Bellato HM, Hajj GN. 2016. Translational control by eIF2alpha in neurons: beyond the stress response. Cytoskeleton 73:551–565. https://doi.org/10.1002/cm.21294.
23. Garcia-Maurino SM, Rivero-Rodriguez F, Velazquez-Cruz A, Hernandez-Vellisca M, Diaz-Quintana A, De la Rosa MA, Diaz-Moreno I. 2017. RNA binding protein regulation and cross-talk in the control of AU-rich mRNA fate. Front Mol Biosci 4:71. https://doi.org/10.3389/fmolb.2017.00071.
24. Meyuhas O, Kahan T. 2015. The race to decipher the top secrets of TOP mRNAs. Biochim Biophys Acta 1849:801–811. https://doi.org/10.1016/j.bbagrm.2014.08.015.
25. Hinnebusch AG, Ivanov IP, Sonenberg N. 2016. Translational control by 5′-untranslated regions of eukaryotic mRNAs. Science 352:1413–1416. https://doi.org/10.1126/science.aad9868.
26. Gingras AC, Gygi SP, Raught B, Polakiewicz RD, Abraham RT, Hoekstra MF, Aebersold R, Sonenberg N. 1999. Regulation of 4E-BP1 phosphorylation: a novel two-step mechanism. Genes Dev 13:1422–1437. https://doi.org/10.1101/gad.13.11.1422.
27. Pause A, Belsham GJ, Gingras AC, Donze O, Lin TA, Lawrence JC, Jr, Sonenberg N. 1994. Insulin-dependent stimulation of protein synthesis by phosphorylation of a regulator of 5′-cap function. Nature 371:762–767. https://doi.org/10.1038/371762a0.
28. Lin TA, Kong X, Saltiel AR, Blackshear PJ, Lawrence JC, Jr. 1995. Control of PHAS-I by insulin in 3T3-L1 adipocytes. Synthesis, degradation, and phosphorylation by a rapamycin-sensitive and mitogen-activated protein kinase-independent pathway. J Biol Chem 270:18531–18538. https://doi.org/10.1074/jbc.270.31.18531.
29. Gingras AC, Raught B, Gygi SP, Niedzwiecka A, Miron M, Burley SK, Polakiewicz RD, Wyslouch-Cieszynska A, Aebersold R, Sonenberg N. 2001. Hierarchical phosphorylation of the translation inhibitor 4E-BP1. Genes Dev 15:2852–2864. https://doi.org/10.1101/gad.887201.
30. Piccirillo CA, Bjur E, Topisirovic I, Sonenberg N, Larsson O. 2014. Translational control of immune responses: from transcripts to translatomes. Nat Immunol 15:503–511. https://doi.org/10.1038/ni.2891.
31. Mohr I, Sonenberg N. 2012. Host translation at the nexus of infection and immunity. Cell Host Microbe 12:470–483. https://doi.org/10.1016/j.chom.2012.09.006.
32. Walsh D, Mathews MB, Mohr I. 2013. Tinkering with translation: protein synthesis in virus-infected cells. Cold Spring Harb Perspect Biol 5:a012351. https://doi.org/10.1101/cshperspect.a012351.
33. Kaur S, Lal L, Sassano A, Majchrzak-Kita B, Srikanth M, Baker DP, Petroulakis E, Hay N, Sonenberg N, Fish EN, Platanias LC. 2007. Regulatory effects of mammalian target of rapamycin-activated pathways in type I and II interferon signaling. J Biol Chem 282:1757–1768. https://doi.org/10.1074/jbc.M607365200.
34. Cao W, Manicassamy S, Tang H, Kasturi SP, Pirani A, Murthy N, Pulendran B. 2008. Toll-like receptor-mediated induction of type I interferon in plasmacytoid dendritic cells requires the rapamycin-sensitive PI(3)K-mTOR-p70S6K pathway. Nat Immunol 9:1157–1164. https://doi.org/10.1038/ni.1645.
35. Costa-Mattioli M, Sonenberg N. 2008. RAPping production of type I interferon in pDCs through mTOR. Nat Immunol 9:1097–1099. https://doi.org/10.1038/ni1008-1097.
36. Alain T, Lun X, Martineau Y, Sean P, Pulendran B, Petroulakis E, Zemp FJ, Lemay CG, Roy D, Bell JC, Thomas G, Kozma SC, Forsyth PA, Costa-Mattioli M, Sonenberg N. 2010. Vesicular stomatitis virus oncolysis is potentiated by impairing mTORC1-dependent type I IFN production. Proc Natl Acad Sci U S A 107:1576–1581. https://doi.org/10.1073/pnas.0912344107.
37. Nehdi A, Sean P, Linares I, Colina R, Jaramillo M, Alain T. 2014. Deficiency

in either 4E-BP1 or 4E-BP2 augments innate antiviral immune responses. PLoS One 9:e114854. https://doi.org/10.1371/journal.pone.0114854.
38. Spangle JM, Munger K. 2010. The human papillomavirus type 16 E6 oncoprotein activates mTORC1 signaling and increases protein synthesis. J Virol 84:9398–9407. https://doi.org/10.1128/JVI.00974-10.
39. Clippinger AJ, Maguire TG, Alwine JC. 2011. The changing role of mTOR kinase in the maintenance of protein synthesis during human cytomegalovirus infection. J Virol 85:3930–3939. https://doi.org/10.1128/JVI.01913-10.
40. Chakrabarti S, Liehl P, Buchon N, Lemaitre B. 2012. Infection-induced host translational blockage inhibits immune responses and epithelial renewal in the *Drosophila* gut. Cell Host Microbe 12:60–70. https://doi.org/10.1016/j.chom.2012.06.001.
41. Sokolova O, Vieth M, Gnad T, Bozko PM, Naumann M. 2014. *Helicobacter pylori* promotes eukaryotic protein translation by activating phosphatidylinositol 3 kinase/mTOR. Int J Biochem Cell Biol 55:157–163. https://doi.org/10.1016/j.biocel.2014.08.023.
42. Jaramillo M, Gomez MA, Larsson O, Shio MT, Topisirovic I, Contreras I, Luxenburg R, Rosenfeld A, Colina R, McMaster RW, Olivier M, Costa-Mattioli M, Sonenberg N. 2011. Leishmania repression of host translation through mTOR cleavage is required for parasite survival and infection. Cell Host Microbe 9:331–341. https://doi.org/10.1016/j.chom.2011.03.008.
43. Holmes MJ, Augusto LDS, Zhang M, Wek RC, Sullivan WJ, Jr. 2017. Translational control in the latency of apicomplexan parasites. Trends Parasitol 33:947–960. https://doi.org/10.1016/j.pt.2017.08.006.
44. Hassan MA, Vasquez JJ, Guo-Liang C, Meissner M, Nicolai Siegel T. 2017. Comparative ribosome profiling uncovers a dominant role for translational control in Toxoplasma gondii. BMC Genomics 18:961. https://doi.org/10.1186/s12864-017-4362-6.
45. Larsson O, Sonenberg N, Nadon R. 2011. anota: analysis of differential translation in genome-wide studies. Bioinformatics 27:1440–1441. https://doi.org/10.1093/bioinformatics/btr146.
46. Kramer A, Green J, Pollard J, Jr, Tugendreich S. 2014. Causal analysis approaches in Ingenuity Pathway Analysis. Bioinformatics 30:523–530. https://doi.org/10.1093/bioinformatics/btt703.
47. O'Leary NA, Wright MW, Brister JR, Ciufo S, Haddad D, McVeigh R, Rajput B, Robbertse B, Smith-White B, Ako-Adjei D, Astashyn A, Badretdin A, Bao Y, Blinkova O, Brover V, Chetvernin V, Choi J, Cox E, Ermolaeva O, Farrell CM, Goldfarb T, Gupta T, Haft D, Hatcher E, Hlavina W, Joardar VS, Kodali VK, Li W, Maglott D, Masterson P, McGarvey KM, Murphy MR, O'Neill K, Pujar S, Rangwala SH, Rausch D, Riddick LD, Schoch C, Shkeda A, Storz SS, Sun H, Thibaud-Nissen F, Tolstoy I, Tully RE, Vatsan AR, Wallin C, Webb D, Wu W, Landrum MJ, Kimchi A, et al. 2016. Reference sequence (RefSeq) database at NCBI: current status, taxonomic expansion, and functional annotation. Nucleic Acids Res 44:D733–D745. https://doi.org/10.1093/nar/gkv1189.
48. Bailey TL, Johnson J, Grant CE, Noble WS. 2015. The MEME suite. Nucleic Acids Res 43:W39–W49. https://doi.org/10.1093/nar/gkv416.
49. Levy S, Avni D, Hariharan N, Perry RP, Meyuhas O. 1991. Oligopyrimidine tract at the 5′ end of mammalian ribosomal protein mRNAs is required for their translational control. Proc Natl Acad Sci U S A 88:3319–3323.
50. Miloslavski R, Cohen E, Avraham A, Iluz Y, Hayouka Z, Kasir J, Mudhasani R, Jones SN, Cybulski N, Ruegg MA, Larsson O, Gandin V, Rajakumar A, Topisirovic I, Meyuhas O. 2014. Oxygen sufficiency controls TOP mRNA translation via the TSC-Rheb-mTOR pathway in a 4E-BP-independent manner. J Mol Cell Biol 6:255–266. https://doi.org/10.1093/jmcb/mju008.
51. Gandin V, Masvidal L, Hulea L, Gravel SP, Cargnello M, McLaughlan S, Cai Y, Balanathan P, Morita M, Rajakumar A, Furic L, Pollak M, Porco JA, Jr, St-Pierre J, Pelletier J, Larsson O, Topisirovic I. 2016. nanoCAGE reveals 5′ UTR features that define specific modes of translation of functionally related MTOR-sensitive mRNAs. Genome Res 26:636–648. https://doi.org/10.1101/gr.197566.115.
52. Masvidal L, Hulea L, Furic L, Topisirovic I, Larsson O. 2017. mTOR-sensitive translation: cleared fog reveals more trees. RNA Biol 14:1299–1305. https://doi.org/10.1080/15476286.2017.1290041.
53. Larsson O, Morita M, Topisirovic I, Alain T, Blouin MJ, Pollak M, Sonenberg N. 2012. Distinct perturbation of the translatome by the antidiabetic drug metformin. Proc Natl Acad Sci U S A 109:8977–8982. https://doi.org/10.1073/pnas.1201689109.
54. Thoreen CC, Kang SA, Chang JW, Liu Q, Zhang J, Gao Y, Reichling LJ, Sim T, Sabatini DM, Gray NS. 2009. An ATP-competitive mammalian target of rapamycin inhibitor reveals rapamycin-resistant functions of mTORC1. J Biol Chem 284:8023–8032. https://doi.org/10.1074/jbc.M900301200.
55. Laplante M, Sabatini DM. 2009. mTOR signaling at a glance. J Cell Sci 122:3589–3594. https://doi.org/10.1242/jcs.051011.
56. Hirai H, Sootome H, Nakatsuru Y, Miyama K, Taguchi S, Tsujioka K, Ueno Y, Hatch H, Majumder PK, Pan BS, Kotani H. 2010. MK-2206, an allosteric Akt inhibitor, enhances antitumor efficacy by standard chemotherapeutic agents or molecular targeted drugs in vitro and in vivo. Mol Cancer Ther 9:1956–1967. https://doi.org/10.1158/1535-7163.MCT-09-1012.
57. Jewell JL, Kim YC, Russell RC, Yu FX, Park HW, Plouffe SW, Tagliabracci VS, Guan KL. 2015. Metabolism. Differential regulation of mTORC1 by leucine and glutamine. Science 347:194–198. https://doi.org/10.1126/science.1259472.
58. Dowling RJ, Topisirovic I, Alain T, Bidinosti M, Fonseca BD, Petroulakis E, Wang X, Larsson O, Selvaraj A, Liu Y, Kozma SC, Thomas G, Sonenberg N. 2010. mTORC1-mediated cell proliferation, but not cell growth, controlled by the 4E-BPs. Science 328:1172–1176. https://doi.org/10.1126/science.1187532.
59. Al-Bajalan MMM, Xia D, Armstrong S, Randle N, Wastling JM. 2017. *Toxoplasma gondii* and *Neospora caninum* induce different host cell responses at proteome-wide phosphorylation events; a step forward for uncovering the biological differences between these closely related parasites. Parasitol Res 10:2707–2719. https://doi.org/10.1007/s00436-017-5579-7.
60. Wang Y, Weiss LM, Orlofsky A. 2009. Intracellular parasitism with *Toxoplasma gondii* stimulates mammalian-target-of-rapamycin-dependent host cell growth despite impaired signalling to S6K1 and 4E-BP1. Cell Microbiol 11:983–1000. https://doi.org/10.1111/j.1462-5822.2009.01305.x.
61. Wang Y, Weiss LM, Orlofsky A. 2009. Host cell autophagy is induced by *Toxoplasma gondii* and contributes to parasite growth. J Biol Chem 284:1694–1701. https://doi.org/10.1074/jbc.M807890200.
62. Wang Y, Weiss LM, Orlofsky A. 2010. Coordinate control of host centrosome position, organelle distribution, and migratory response by *Toxoplasma gondii* via host mTORC2. J Biol Chem 285:15611–15618. https://doi.org/10.1074/jbc.M109.095778.
63. Sancak Y, Bar-Peled L, Zoncu R, Markhard AL, Nada S, Sabatini DM. 2010. Ragulator-Rag complex targets mTORC1 to the lysosomal surface and is necessary for its activation by amino acids. Cell 141:290–303. https://doi.org/10.1016/j.cell.2010.02.024.
64. Xu X, Xiong X, Sun Y. 2016. The role of ribosomal proteins in the regulation of cell proliferation, tumorigenesis, and genomic integrity. Sci China Life Sci 59:656–672. https://doi.org/10.1007/s11427-016-0018-0.
65. Goebel S, Luder CG, Lugert R, Bohne W, Gross U. 1998. *Toxoplasma gondii* inhibits the in vitro induced apoptosis of HL-60 cells. Tokai J Exp Clin Med 23:351–356.
66. Nash PB, Purner MB, Leon RP, Clarke P, Duke RC, Curiel TJ. 1998. *Toxoplasma gondii*-infected cells are resistant to multiple inducers of apoptosis. J Immunol 160:1824–1830.
67. Lavine MD, Arrizabalaga G. 2009. Induction of mitotic S-phase of host and neighboring cells by *Toxoplasma gondii* enhances parasite invasion. Mol Biochem Parasitol 164:95–99. https://doi.org/10.1016/j.molbiopara.2008.11.014.
68. Molestina RE, El-Guendy N, Sinai AP. 2008. Infection with Toxoplasma gondii results in dysregulation of the host cell cycle. Cell Microbiol 10:1153–1165. https://doi.org/10.1111/j.1462-5822.2008.01117.x.
69. Dunay IR, Damatta RA, Fux B, Presti R, Greco S, Colonna M, Sibley LD. 2008. Gr1(+) inflammatory monocytes are required for mucosal resistance to the pathogen *Toxoplasma gondii*. Immunity 29:306–317. https://doi.org/10.1016/j.immuni.2008.05.019.
70. Aliberti J, Reis e Sousa C, Schito M, Hieny S, Wells T, Huffnagle GB, Sher A. 2000. CCR5 provides a signal for microbial induced production of IL-12 by CD8 alpha+ dendritic cells. Nat Immunol 1:83–87. https://doi.org/10.1038/76957.
71. Deckert M, Sedgwick JD, Fischer E, Schluter D. 2006. Regulation of microglial cell responses in murine *Toxoplasma* encephalitis by CD200/CD200 receptor interaction. Acta Neuropathol 111:548–558. https://doi.org/10.1007/s00401-006-0062-z.
72. Morita M, Gravel SP, Chenard V, Sikstrom K, Zheng L, Alain T, Gandin V, Avizonis D, Arguello M, Zakaria C, McLaughlan S, Nouet Y, Pause A, Pollak M, Gottlieb E, Larsson O, St-Pierre J, Topisirovic I, Sonenberg N. 2013. mTORC1 controls mitochondrial activity and biogenesis through

4E-BP-dependent translational regulation. Cell Metab 18:698–711. https://doi.org/10.1016/j.cmet.2013.10.001.
73. Morita M, Prudent J, Basu K, Goyon V, Katsumura S, Hulea L, Pearl D, Siddiqui N, Strack S, McGuirk S, St-Pierre J, Larsson O, Topisirovic I, Vali H, McBride HM, Bergeron JJ, Sonenberg N. 2017. mTOR controls mitochondrial dynamics and cell survival via MTFP1. Mol Cell 67:922.e5–935.e5. https://doi.org/10.1016/j.molcel.2017.08.013.
74. de Melo EJ, de Carvalho TU, de Souza W. 1992. Penetration of Toxoplasma gondii into host cells induces changes in the distribution of the mitochondria and the endoplasmic reticulum. Cell Struct Funct 17:311–317. https://doi.org/10.1247/csf.17.311.
75. Lindsay DS, Mitschler RR, Toivio-Kinnucan MA, Upton SJ, Dubey JP, Blagburn BL. 1993. Association of host cell mitochondria with developing *Toxoplasma gondii* tissue cysts. Am J Vet Res 54:1663–1667.
76. Sinai AP, Joiner KA. 2001. The *Toxoplasma gondii* protein ROP2 mediates host organelle association with the parasitophorous vacuole membrane. J Cell Biol 154:95–108. https://doi.org/10.1083/jcb.200101073.
77. Sinai AP, Webster P, Joiner KA. 1997. Association of host cell endoplasmic reticulum and mitochondria with the *Toxoplasma gondii* parasitophorous vacuole membrane: a high affinity interaction. J Cell Sci 110(Part 17):2117–2128.
78. Syn G, Anderson D, Blackwell JM, Jamieson SE. 2017. *Toxoplasma gondii* infection is associated with mitochondrial dysfunction in-vitro. Front Cell Infect Microbiol 7:512. https://doi.org/10.3389/fcimb.2017.00512.
79. Pernas L, Adomako-Ankomah Y, Shastri AJ, Ewald SE, Treeck M, Boyle JP, Boothroyd JC. 2014. *Toxoplasma* effector MAF1 mediates recruitment of host mitochondria and impacts the host response. PLoS Biol 12:e1001845. https://doi.org/10.1371/journal.pbio.1001845.
80. Sorensen SW, Billington CJ, Norris SA, Briggs JE, Reding MT, Filice GA. 1997. *Toxoplasma gondii*: metabolism of intracellular tachyzoites is affected by host cell ATP production. Exp Parasitol 85:101–104. https://doi.org/10.1006/expr.1996.4128.
81. Silverman JA, Qi H, Riehl A, Beckers C, Nakaar V, Joiner KA. 1998. Induced activation of the *Toxoplasma gondii* nucleoside triphosphate hydrolase leads to depletion of host cell ATP levels and rapid exit of intracellular parasites from infected cells. J Biol Chem 273:12352–12359. https://doi.org/10.1074/jbc.273.20.12352.
82. Coppens I. 2017. How *Toxoplasma* and malaria parasites defy first, then exploit host autophagic and endocytic pathways for growth. Curr Opin Microbiol 40:32–39. https://doi.org/10.1016/j.mib.2017.10.009.
83. Saeij JP, Frickel EM. 2017. Exposing *Toxoplasma gondii* hiding inside the vacuole: a role for GBPs, autophagy and host cell death. Curr Opin Microbiol 40:72–80. https://doi.org/10.1016/j.mib.2017.10.021.
84. Kimura T, Jain A, Choi SW, Mandell MA, Schroder K, Johansen T, Deretic V. 2015. TRIM-mediated precision autophagy targets cytoplasmic regulators of innate immunity. J Cell Biol 210:973–989. https://doi.org/10.1083/jcb.201503023.
85. Ewald SE, Chavarria-Smith J, Boothroyd JC. 2014. NLRP1 is an inflammasome sensor for *Toxoplasma gondii*. Infect Immun 82:460–468. https://doi.org/10.1128/IAI.01170-13.
86. Gorfu G, Cirelli KM, Melo MB, Mayer-Barber K, Crown D, Koller BH, Masters S, Sher A, Leppla SH, Moayeri M, Saeij JP, Grigg ME. 2014. Dual role for inflammasome sensors NLRP1 and NLRP3 in murine resistance to *Toxoplasma gondii*. mBio 5:e01117-13. https://doi.org/10.1128/mBio.01117-13.
87. Hermanns T, Muller UB, Konen-Waisman S, Howard JC, Steinfeldt T. 2016. The *Toxoplasma gondii* rhoptry protein ROP18 is an Irga6-specific kinase and regulated by the dense granule protein GRA7. Cell Microbiol 18:244–259. https://doi.org/10.1111/cmi.12499.
88. Fentress SJ, Behnke MS, Dunay IR, Mashayekhi M, Rommereim LM, Fox BA, Bzik DJ, Taylor GA, Turk BE, Lichti CF, Townsend RR, Qiu W, Hui R, Beatty WL, Sibley LD. 2010. Phosphorylation of immunity-related GTPases by a *Toxoplasma gondii*-secreted kinase promotes macrophage survival and virulence. Cell Host Microbe 8:484–495. https://doi.org/10.1016/j.chom.2010.11.005.
89. Steinfeldt T, Konen-Waisman S, Tong L, Pawlowski N, Lamkemeyer T, Sibley LD, Hunn JP, Howard JC. 2010. Phosphorylation of mouse immunity-related GTPase (IRG) resistance proteins is an evasion strategy for virulent *Toxoplasma gondii*. PLoS Biol 8:e1000576. https://doi.org/10.1371/journal.pbio.1000576.
90. Foltz C, Napolitano A, Khan R, Clough B, Hirst EM, Frickel EM. 2017. TRIM21 is critical for survival of *Toxoplasma gondii* infection and localises to GBP-positive parasite vacuoles. Sci Rep 7:5209. https://doi.org/10.1038/s41598-017-05487-7.
91. Babendure JR, Babendure JL, Ding JH, Tsien RY. 2006. Control of mammalian translation by mRNA structure near caps. RNA 12:851–861. https://doi.org/10.1261/rna.2309906.
92. Jenkins RH, Bennagi R, Martin J, Phillips AO, Redman JE, Fraser DJ. 2010. A conserved stem loop motif in the 5′untranslated region regulates transforming growth factor-beta(1) translation. PLoS One 5:e12283. https://doi.org/10.1371/journal.pone.0012283.
93. Leung AK, Sharp PA. 2010. MicroRNA functions in stress responses. Mol Cell 40:205–215. https://doi.org/10.1016/j.molcel.2010.09.027.
94. Liu B, Qian SB. 2014. Translational reprogramming in cellular stress response. Wiley Interdiscip Rev RNA 5:301–315. https://doi.org/10.1002/wrna.1212.
95. Landry DM, Hertz MI, Thompson SR. 2009. RPS25 is essential for translation initiation by the Dicistroviridae and hepatitis C viral IRESs. Genes Dev 23:2753–2764. https://doi.org/10.1101/gad.1832209.
96. Fischer K, Roberts M, Roscoe S, Avci Y, Ananvoranich S. 2018. *Toxoplasma gondii* infection induces the formation of host's nuclear granules containing poly(A)-binding proteins. Can J Microbiol https://doi.org/10.1139/cjm-2017-0755.
97. Goss DJ, Kleiman FE. 2013. Poly(A) binding proteins: are they all created equal? Wiley Interdiscip Rev RNA 4:167–179. https://doi.org/10.1002/wrna.1151.
98. Smith RW, Blee TK, Gray NK. 2014. Poly(A)-binding proteins are required for diverse biological processes in metazoans. Biochem Soc Trans 42:1229–1237. https://doi.org/10.1042/BST20140111.
99. Eliseeva IA, Lyabin DN, Ovchinnikov LP. 2013. Poly(A)-binding proteins: structure, domain organization, and activity regulation. Biochemistry 78:1377–1391. https://doi.org/10.1134/S0006297913130014.
100. Nelson MM, Jones AR, Carmen JC, Sinai AP, Burchmore R, Wastling JM. 2008. Modulation of the host cell proteome by the intracellular apicomplexan parasite *Toxoplasma gondii*. Infect Immun 76:828–844. https://doi.org/10.1128/IAI.01115-07.
101. Leroux LP, Nishi M, El-Hage S, Fox BA, Bzik DJ, Dzierszinski FS. 2015. Parasite manipulation of the invariant chain and the peptide editor H2-DM affects major histocompatibility complex class II antigen presentation during *Toxoplasma gondii* infection. Infect Immun 83:3865–3880. https://doi.org/10.1128/IAI.00415-15.
102. Lau YL, Lee WC, Gudimella R, Zhang G, Ching XT, Razali R, Aziz F, Anwar A, Fong MY. 2016. Deciphering the draft genome of *Toxoplasma gondii* RH strain. PLoS One 11:e0157901. https://doi.org/10.1371/journal.pone.0157901.
103. Kim D, Langmead B, Salzberg SL. 2015. HISAT: a fast spliced aligner with low memory requirements. Nat Methods 12:357–360. https://doi.org/10.1038/nmeth.3317.
104. Ramskold D, Wang ET, Burge CB, Sandberg R. 2009. An abundance of ubiquitously expressed genes revealed by tissue transcriptome sequence data. PLoS Comput Biol 5:e1000598. https://doi.org/10.1371/journal.pcbi.1000598.
105. Ritchie ME, Phipson B, Wu D, Hu Y, Law CW, Shi W, Smyth GK. 2015. limma powers differential expression analyses for RNA-sequencing and microarray studies. Nucleic Acids Res 43:e47. https://doi.org/10.1093/nar/gkv007.
106. Larsson O, Sonenberg N, Nadon R. 2010. Identification of differential translation in genome wide studies. Proc Natl Acad Sci U S A 107:21487–21492. https://doi.org/10.1073/pnas.1006821107.
107. Thoreen CC, Chantranupong L, Keys HR, Wang T, Gray NS, Sabatini DM. 2012. A unifying model for mTORC1-mediated regulation of mRNA translation. Nature 485:109–113. https://doi.org/10.1038/nature11083.
108. Nickles D, Sandmann T, Ziman R, Bourgon R. 2017. NanoStringQCPro: quality metrics and data processing methods for NanoString mRNA gene expression data. R package version 1.10.0.
109. Dzitko K, Dudzinska D, Grzybowski M, Dlugonska H. 2010. The utility of MTT and XTT colorimetric tests in the studies conducted in vitro with *Toxoplasma gondii* tachyzoites. Wiad Parazytol 56:145–152. (In Polish.)
110. Weiss LM, Kim K. 2007. *Toxoplasma gondii*: the model apicomplexan. Perspectives and methods, 1st ed. Elsevier/Academic Press, Boston, MA.
111. Schindelin J, Arganda-Carreras I, Frise E, Kaynig V, Longair M, Pietzsch T, Preibisch S, Rueden C, Saalfeld S, Schmid B, Tinevez JY, White DJ, Hartenstein V, Eliceiri K, Tomancak P, Cardona A. 2012. Fiji: an open-source platform for biological-image analysis. Nat Methods 9:676–682. https://doi.org/10.1038/nmeth.2019.
112. Livak KJ, Schmittgen TD. 2001. Analysis of relative gene expression data using real-time quantitative PCR and the 2(−Delta Delta C(T)) method. Methods 25:402–408. https://doi.org/10.1006/meth.2001.1262.